1980

Petrology and uranium mineralization of the Idaho batholith near Stanley Custer County Idaho

Elise L. Erler
The University of Montana

PETROLOGY AND URANIUM MINERALIZATION OF THE IDAHO BATHOLITH NEAR STANLEY, CUSTER COUNTY, IDAHO

by

Elise L. Erler

A.B., Dartmouth College, 1976

Presented in partial fulfillment of the requirements for the degree of

Master of Science

UNIVERSITY OF MONTANA

1980

Approved by:

Donald W. Hyndman
Chairman, Board of Examiners

Dean, Graduate School

6/3/80
Date

ABSTRACT

Erler, Elise L., M.S., Spring, 1980 Geology

Petrology and Uranium Mineralization of the Idaho Batholith near Stanley, Custer County, Idaho (98 pp.)

Director: Donald W. Hyndman DWH

The Cretaceous Idaho batholith hosts uranium mineralization in the Basin Creek area, approximately 15 km northeast of Stanley, Idaho. Five rock types are locally present within the batholith: 1) biotite-bearing equigranular granite, 2) biotite-bearing quartz granite porphyry, 3) biotite-bearing K-feldspar porphyritic granite, 4) biotite-bearing leucocratic granite, and 5) granitic aplite and pegmatite dikes. Field relationships indicate that the equigranular granite is an early unit of the batholith. Quartz granite porphyry and slightly younger K-feldspar porphyritic granite were emplaced later than the equigranular granite. The porphyritic granites are similar in appearance except for the development of 1-8 cm-long K-feldspar megacrysts within the K-feldspar porphyritic granite. These granite magmas may have been differentiates of the equigranular granite magma or the product of a different magma. The leucocratic granite is a late-stage differentiate of the Idaho batholith, similar in appearance to the White Cloud stock, 20 km south. Numerous granitic pegmatites and aplites cut the three older units of the batholith along a northwest-trending structural grain.

Quartz granite porphyry and K-feldspar porphyritic granite host three types of uranium mineralization: 1) uraninite in chalcedony veins, 2) stockwork uraninite in locally concentrated, small tension shears, and 3) uranophane and autunite in pegmatites. Leucocratic granite has low radioactivity and no uranium occurrences. Uranium either was introduced prior to intrusion of the leucocratic granite as magma-derived late-stage volatiles that escaped along zones of weakness to form pegmatites, aplites, and uraniferous veins or was associated with the Eocene igneous activity of the Challis volcanics forming supergene or hypogene uranium deposits.

ACKNOWLEDGMENTS

It is not possible to name all the people who have assisted me with this study. However, some have been outstanding with their encouragement, enthusiasm, and knowledge of adjacent regions which they shared freely. These include by advisor, Don Hyndman, David Obolewicz of the Anaconda Copper Company, and Earl Bennett of the Idaho Bureau of Mines and Geology. Others who have contributed considerable time and effort are David Fountain, Ian Lange, and Ken Watson. My colleagues Bill Beyer, Carleen Holloway, and Charlie Rubin provided endless advice and moral support.

Financial and logistical support were provided by Noranda Exploration, Inc. and are gratefully acknowledged.

TABLE OF CONTENTS

TABLE OF CONTENTS (continued)

TABLE OF CONTENTS (continued)

LIST OF FIGURES

LIST OF FIGURES (continued)

LIST OF PLATES

LIST OF TABLES

CHAPTER I

INTRODUCTION

The Basin Creek area lies along the eastern edge of the Atlanta lobe of the Idaho batholith at $114^{o}52'30''$ west longitude and $44^{o}17'$ north latitude (Figure 1). In this area Cretaceous granitic rocks containing xenoliths of Paleozoic metasedimentary rocks are overlain by Tertiary volcanics. During Mesozoic time, a series of mesozonal intrusions formed the Idaho batholith within a regionally metamorphosed Paleozoic to Precambrian sedimentary package. Following uplift and erosion in early Tertiary time, the Challis volcanics were deposited on top of and within both the intrusive and metamorphic rocks.

Within this geologic framework, uranium was deposited in the Basin Creek area in the Cretaceous intrusive rocks and in an early Tertiary arkose unconformably overlying the Idaho batholith. The purpose of this study was to interpret the petrology of the granitic rocks and associated mineralization in order to determine if there is a genetic relationship between the granite and uranium mineralization.

LOCATION AND ACCESS

The Basin Creek area lies 12 kilometers northeast of Stanley, Idaho and is located north of the Salmon River (Figure 2). The study area (Plate I and Figure 5) is bounded by the Challis volcanics on the northeast, American Creek on the east, the Salmon River on the south, Copper Creek and Potato Mountain on the west, and Little Basin Creek on the north. The study area and the uranium occurrences are centered on

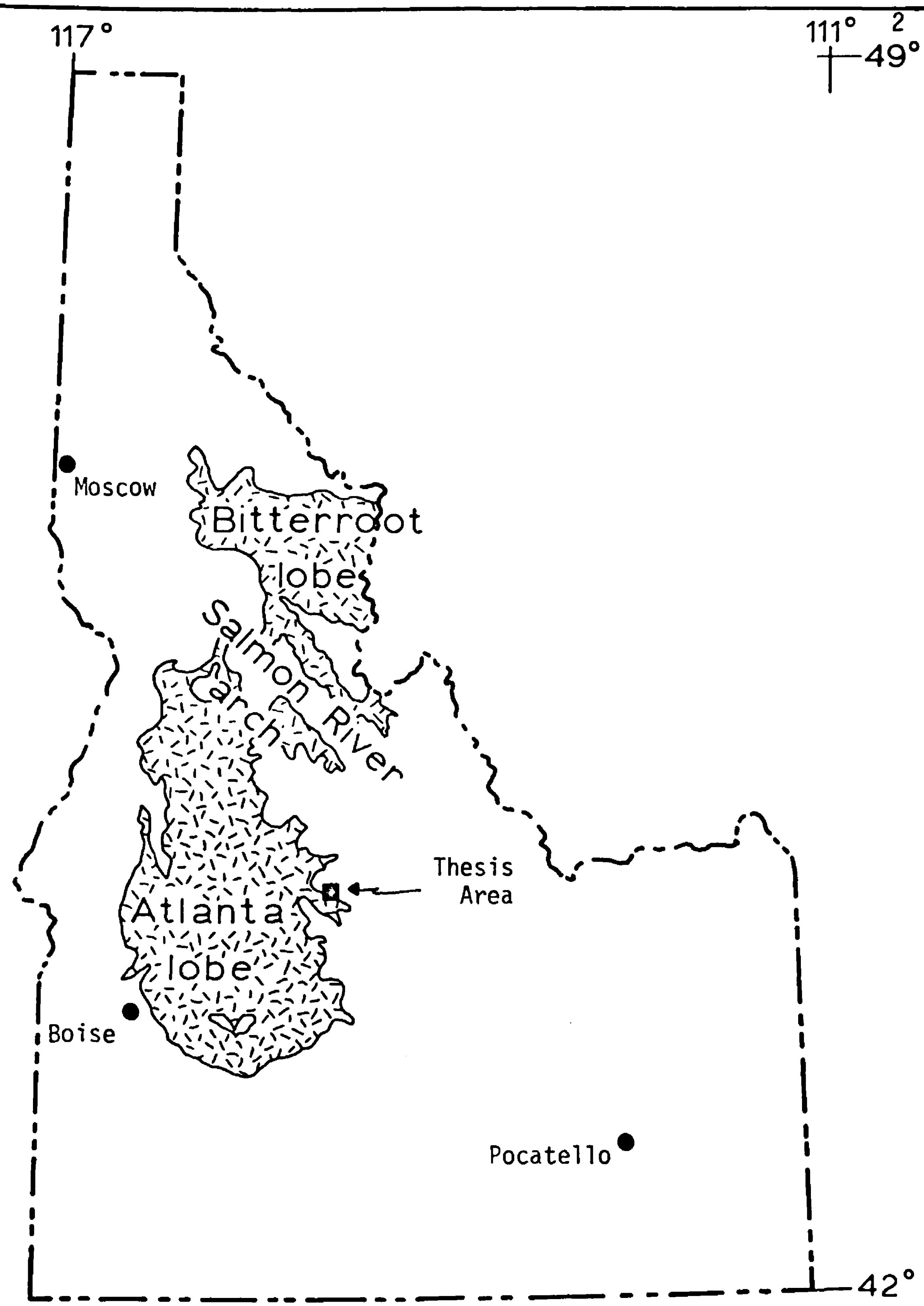

Figure 1. Map of Idaho showing the Idaho batholith and location of the thesis area.

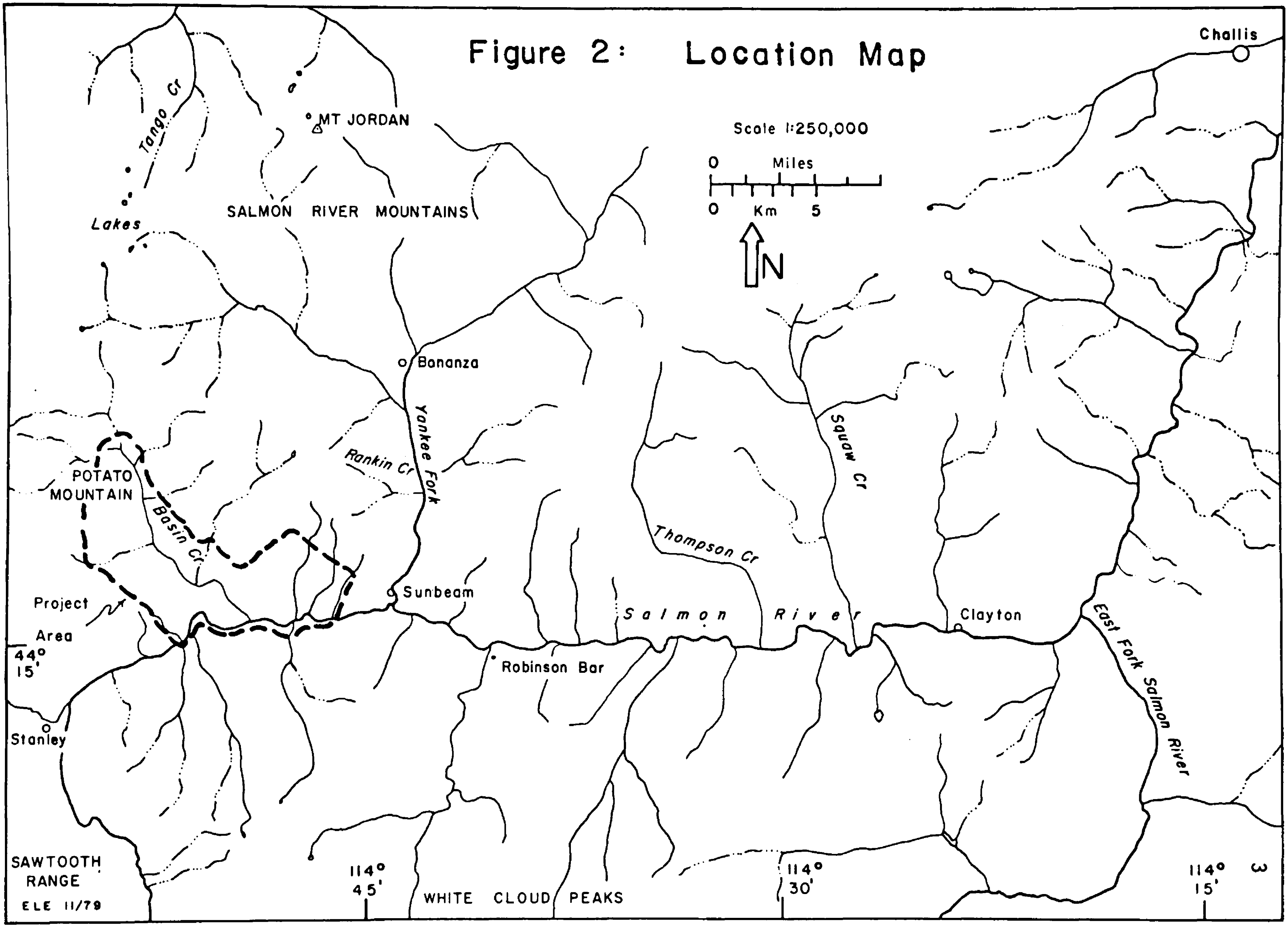

Figure 2: Location Map

Basin Creek which drains into the Salmon River 12.5 kilometers northeast of Stanley. Outcrop is limited in the area; 10% is average with none on the tree-covered north slopes. The best exposures are found along the rapidly downcutting Salmon River.

Access is excellent during the summer and fall months. Idaho Highway 75 (formerly U.S. 93) follows the Salmon River from Challis to Stanley and is kept open all year. Good dirt roads are found up the major drainages to most uranium prospects; logging roads and four-wheel drive trails provide access to the remainder of the thesis area.

PRESENT STUDY

During the summer and fall of 1979, I spent four-and-one-half months in the field preparing a geologic map, gathering samples for chemical analyses and age dates, and collecting hand specimens. Additional geologic work was done for Noranda Exploration, Inc. The base map is a composite of two U.S. Geological Survey 7.5' topographic maps (Basin Butte and East Basin Creek); reconnaissance geologic mapping was done with the aid of aerial photographs at a scale of 1:24,000. Thin sections from selected hand specimens were examined using a petrographic microscope. Modal estimates of composition were made by 2000 point counts on ten samples and by visual estimates on 55 samples. CIPW normative estimates were calculated from whole rock chemical analyses determined by emission spectroscopy. Uranium analyses were determined by qualitative gamma-ray spectrometry.

CHAPTER II

REGIONAL GEOLOGY

LITHOLOGIES

The thesis area is located at the contact of the Idaho batholith and the overlying Eocene Challis volcanics. Exposures of Paleozoic metasedimentary and Precambrian(?) rocks are found within the region. Eocene intrusive bodies are exposed in the general area. Figure 3 shows the regional geology.

Precambrian(?) Rocks

The oldest known rocks to crop out in the Stanley area are metamorphic rocks of the Thompson Peak Formation (Reid, 1963). These rocks are found southwest of the town of Stanley along the eastern edge of the Sawtooth Mountains. Feldspathic schist, feldspar-rich granofels, and lime-silicate granofels make up the mass of Thompson Peak and xenoliths locally within the Idaho batholith. Reid considers these metamorphic rocks, which show more complex deformation and higher-grade metamorphism than nearby Paleozoic sedimentary rocks, to be Precambrian in age because of their similarity to the Wallace Formation of the Proterozoic Belt Supergroup in northern Idaho.

Paleozoic Metasedimentary Rocks

Quartzites, argillites, and silicified limestones of the Pennsylvanian Wood River Formation (Umpleby and others, 1930; Choate, 1962) crop out in the Basin Creek Region. Rocks thought to be Wood

Figure 3: Generalized regional geologic map (modified from Rember and Bennett, 1979).

EXPLANATION

Quaternary sedimentary deposits

Tertiary plutons

Tertiary Challis volcanics

Cretaceous Idaho batholith

Paleozoic metasedimentary rocks

Thesis area

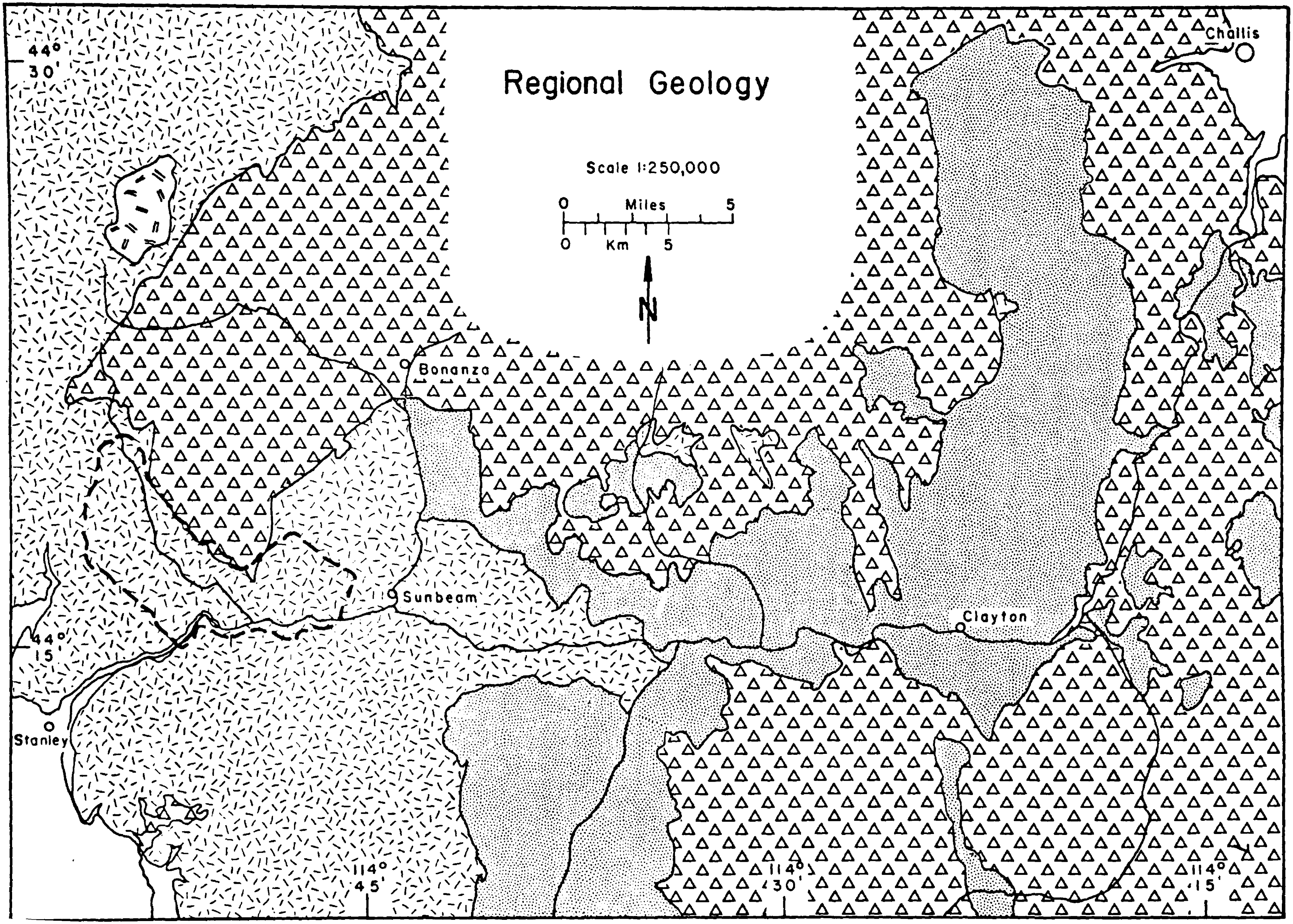

Regional Geology
Scale 1:250,000
0 Miles 5
0 Km 5
N
Challis
Bonanza
Sunbeam
Clayton
Stanley
44°
30'
44°
15'
114°
45'
114°
30'
114°
15'

River Formation are exposed immediately west of the Basin Creek-Salmon River confluence, in the headwaters of American Creek and Rankin Creek, and along the Yankee Fork drainage a few kilometers north of Sunbeam. These rocks probably represent erosional remnants of Paleozoic roof pendants along the eastern margin of the Idaho batholith. The eastern margin of the batholith is exposed along the Salmon River to the west of Slate Creek. Pendants of Paleozoic rocks are well exposed in the White Cloud Peaks south of the thesis area (Bennett, 1973).

Idaho Batholith

Much of the Stanley area is underlain by plutonic rocks of the Atlanta lobe of the Cretaceous Idaho batholith. Potassium-argon dates for plutonic rocks collected near Sunbeam and Robinson Bar along Idaho Highway 75 are approximately 80 million years (m.y.) old (Armstrong, 1975a). Compositional and textural variations of plutonic rocks in the Basin Creek area are diverse (Choate, 1962). Compositions range from sodic granite to calcic granodiorite. Textural variations range from fine- and medium-grained varieties to striking porphyritic textures caused by large crystals of K-feldspar and/or quartz. Numerous pegmatites and aplites cut the batholith in the area.

Two Late Cretaceous stocks are found in the region. The Thompson Creek and White Cloud stocks are leucocratic granites which host sizable molybdenum deposits. Mineralization within the Thompson Creek stock has potassium-argon mica dates of 85.9 ± 3.0 m.y. (muscovite) and 86.9 ± 3.0 m.y. (biotite) (Marvin and others, 1973), placing a lower age limit on the stock. The composite White Cloud stock has a potassium-argon biotite date of 83.6 ± 2.8 m.y. (Seeland, written communication, 1977 in Cavanaugh, 1979). A leucocratic granite unit similar to the White Cloud stock crops out in the thesis area.

Challis Volcanics

Rocks of Tertiary age overlie the Paleozoic and Cretaceous rocks in the Basin Creek area. Ross (1934, 1937) indicated that these rocks comprise the Challis volcanics which he locally subdivided into three members (Figure 4). The Challis volcanics are mainly flows and flow breccias of a wide compositional range with local interbeds of tuffs and sedimentary rocks (Ross, 1961). Potassium-argon dates of the Challis volcanics (Armstrong, 1975a) indicate that most of the volcanics were erupted 54 to 38 m.y. ago.

Plutons of Eocene age are scattered throughout the Idaho batholith (Bond, 1978; Bennett, 1980). In the Stanley area, two such plutons are exposed: the Sawtooth batholith which yields concordant potassium-argon dates of about 44 m.y. (Armstrong, 1974), and the Knapp Peak stock. Both plutonic bodies display features typical of shallow emplacement: miarolitic cavities, smoky quartz, and porphyritic texture (Bennett, 1980).

TECTONIC SETTING

The mesozonal to catazonal Idaho batholith was emplaced into a broad, probably Mesozoic high-grade regional metamorphic terrane (Hyndman, 1979a) of upper Precambrian Belt Supergroup sedimentary rocks and older granitoid orthogneiss (Wiswall, 1979). Hyndman (1979b)

Figure 4: Schematic stratigraphic column of the Challis volcanics (after Ross, 1937).

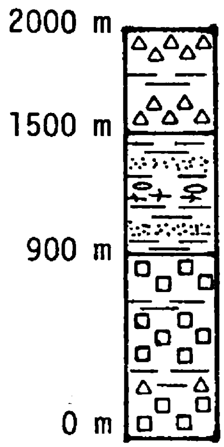

Yankee Fork member: rhyolite flows interbedded with tuffaceous strata.

Germer tuffaceous member: tuff, tuffaceous sandstone, and subordinate amounts of conglomerate and shale; locally fossiliferous; basalt flows locally intercalated.

Latite-andesite member: latite and andesite flows with some intercalated beds of tuff, rhyolite, and basalt flows.

summarizes the tectonic setting of the Idaho batholith, which lies more than 600 kilometers from the present Pacific coastline. This is in contrast to two similar batholiths lying 150 to 200 kilometers east of the coast: the Sierra Nevada batholith of California, and the Coast Range plutonic complex of British Columbia. This anomalous position of the Idaho batholith is off the trend of circum-Pacific batholiths (Hyndman, 1972). The Idaho batholith lies at the eastern end of the Columbia arc which encloses a large region of Miocene Columbia River basalts and no rocks older than Tertiary age. The eastern part of the Columbia arc, in central Oregon, is marked by the Blue Mountain province, a Mesozoic suite of ocean-floor ultramafic rocks, mafic volcanics, and metamorphosed sedimentary rocks. This province extends northeast to the Seven Devils volcanics at the western margin of the Idaho batholith. The Triassic Seven Devils arc-volcanic pile consists of basaltic and andesitic submarine lavas and agglomerates (Vallier, 1977) cut by east-dipping thrust faults. The Seven Devils volcanics are probably a remnant of Mesozoic subduction along the continental margin (Talbot and Hyndman, 1975; Hamilton, 1976). The juxtaposition of this Triassic volcanic arc adjacent to Precambrian crustal rocks to the east around the Idaho batholith with no intervening Paleozoic rocks suggests that the Blue Mountains—Seven Devils block may have moved into place from elsewhere (Hamilton, 1976).

East of the Seven Devils volcanics are extensive Proterozoic Belt metasedimentary rocks and underlying pre-Belt basement rocks, into which the Idaho batholith was emplaced. The batholith is geographically divided into two parts: the northern Bitterroot and southern Atlanta lobes (Figure 1). The two lobes are separated by the southeast-trending Salmon River arch of regionally metamorphosed Belt and pre-Belt rocks (Armstrong, 1975b). Country rocks of the Atlanta lobe on the north and northeast are Belt and pre-Belt basement schists and gneisses; on the east, country rocks are locally Precambrian (?) metamorphic rocks (Dover, 1969; Reid, 1963), and regionally, Devonian to Permian marine clastic rocks are thrust eastward away from the batholith. Along the western margin, the country rocks are metamorphosed submarine volcanics of probable Permo-Triassic age. Large expanses of the Atlanta lobe-country rock contacts are covered by younger rocks, predominantly Tertiary continental volcanic rocks. Miocene Columbia River flood basalts and Pliocene fluvial and lacustrine sediments occur west of the Atlanta lobe; on the south are Pliocene welded tuffs and Pleistocene Snake River Plain flood basalts; and on the east are the Eocene Challis volcanics and related shallow plutons (Bond, 1978).

In the Stanley region, structural features older than Tertiary age are obscured by Eocene and younger tectonic activity. In the Basin Creek area, trap-door tilting of a subsided block of Challis volcanics has thickened the volcanic sequence to the northeast (Siems and others, 1979). This volcanic block is surrounded on all sides except the north-east by the Cretaceous Idaho batholith and the Pennsylvanian Wood River Formation. Parallel northeast trends are seen in the early Tertiary dike swarm (Hyndman and others, 1977) and in the long axis of the Eocene Casto pluton (Siems and others, 1979). Late Cenozoic extension within the Basin and Range province south of the Idaho batholith (Christiansen and Lipman, 1972) is probably responsible for the normal, range-bounding faults which form the Sawtooth Mountains and the Lost River and Pahsimeroi Ranges to the east. An east-northeast trend of hot springs parallels the Salmon River between Stanley and Challis.

Figure 5: Generalized geologic map of the Basin Creek area, Custer County, Idaho.

E X P L A N A T I O N

<u>Quaternary</u>

Alluvium

<u>Tertiary</u>

Silicic dike

Rhyolite

Volcanics- undivided

Arkose

<u>Cretaceous</u>

Leucocratic granite

K-feldspar porphyritic granite

Quartz granite porphyry

Equigranular granite

<u>Paleozoic</u>

Xenolith

S Y M B O L S

Fault

Contact

Topographic high point

Base from U. S. Forest Service map: Custer, NW, quadrangle. (Scale 1:31,680)

Generalized Geology of the Basin Creek Area

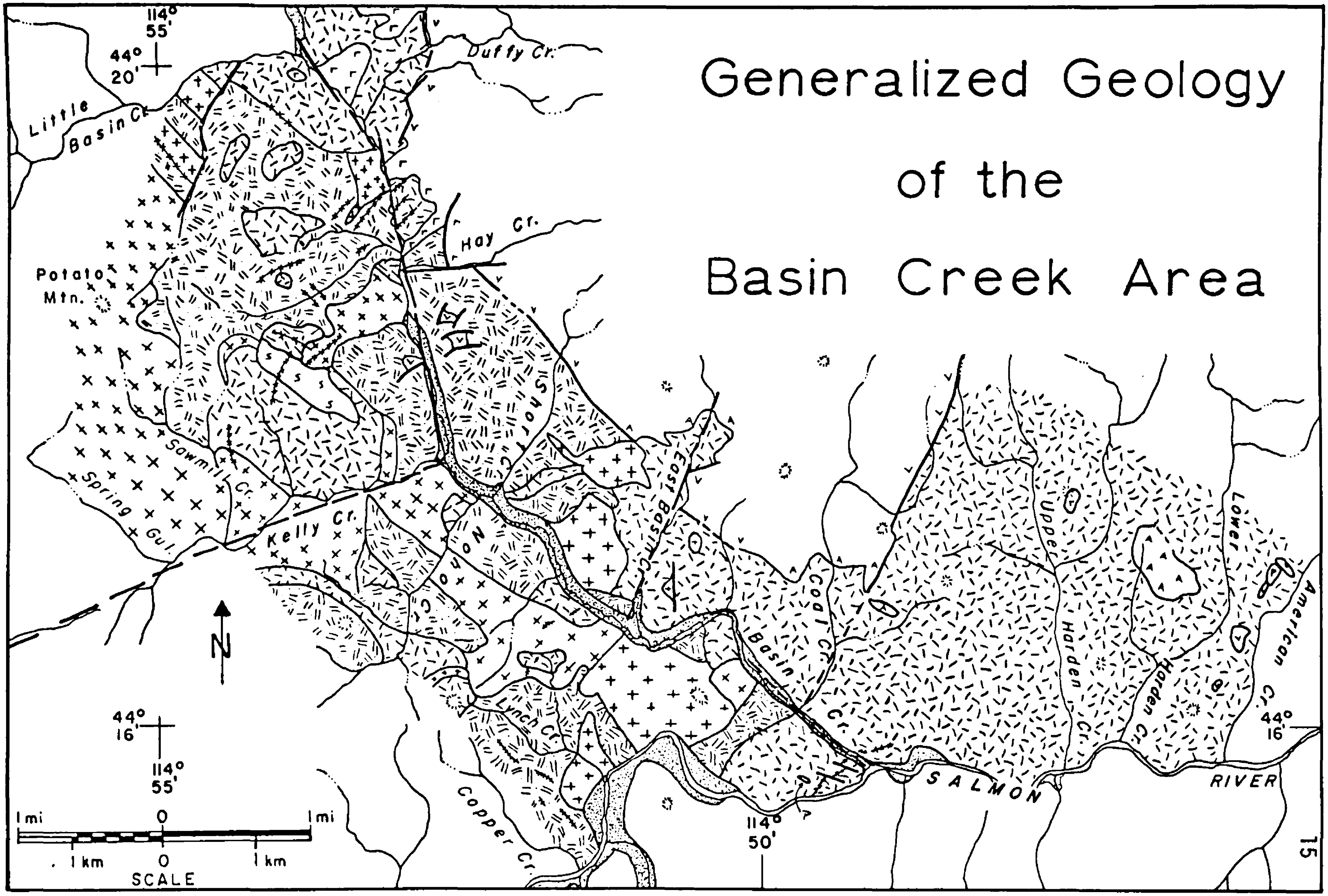

CHAPTER III

GEOLOGY OF THE BASIN CREEK AREA

Geologic mapping divided the plutonic rocks into several textural and compositional phases. The geologic map of the Basin Creek area (Plate I) shows: 1) the distribution of phases of the Idaho batholith, and 2) the spatial relationship of mineralization to phases of the batholith. Figure 5 shows a generalized geologic map of the thesis area. Each geologically important unit is described from both hand specimen and thin section. Point counts were made to accurately determine mineral percentages for at least one thin section from each Cretaceous unit.

CRETACEOUS GRANITIC ROCKS

The Idaho batholith was subdivided into four textural and compositional units. Composition for each unit ranges from granite to granodiorite, but the textures are distinctive for each unit; porphyritic to equigranular. Mineralogical variations control the composition of the rocks; the IUGS classification and nomenclature for plutonic rocks (Streckeisen, 1976) are used to name rocks and are shown in Figure 6.

Equigranular Granite

The oldest Cretaceous granitic unit is an equigranular mafic-bearing phase which crops out over 20% of the thesis area. All other units cut this early phase of the Idaho batholith. Equigranular granite is found only west of Basin Creek. The rock forms small, weathered

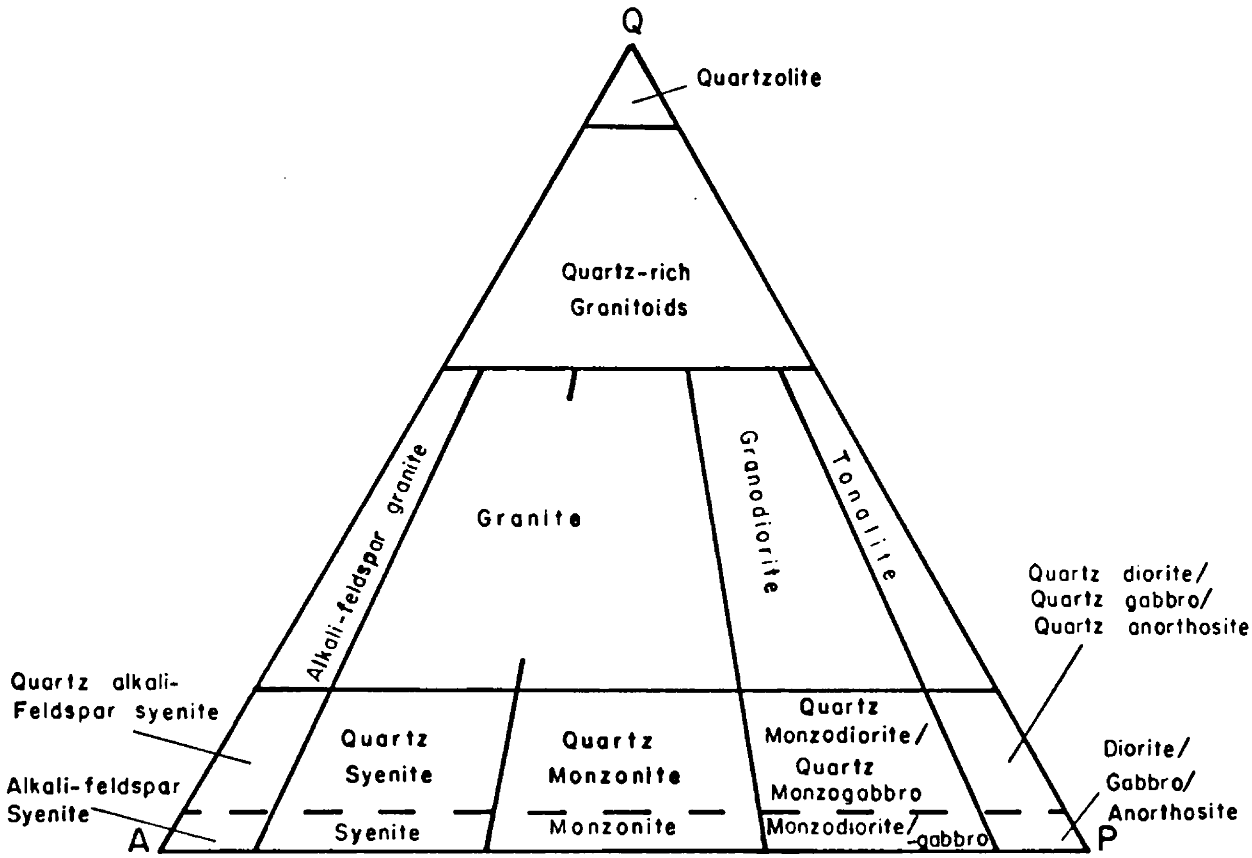

Figure 6: General classification and nomenclature of quartz-bearing plutonic rocks according to mineral content (in volume percent), after Streckeisen (1976, p. 8).

Table 1. Mineralogy and average visual estimate of modes from thin sections of the Cretaceous granitic units in the thesis area.

	K-feldspar	quartz	plagioclase	An (content)	biotite	opaques	apatite	sphene	zircon	hornblende	Alteration minerals present:	white micas	chlorite	iron oxides	carbonate
Equigranular granite	26	30	37	(27)	4	0.7	t	t	t	-		x	x	x	-
Quartz granite porphyry	19	31	40	(30)	6	1	t	t	-	-		x	-	x	x
K-feldspar porphyritic granite	28	29	34	(25)	8	t	t	t	t	t		x	x	x	x
Leucocratic granite	30	33	34	(24)	2	t	t	t	t	-		x	x	x	x

outcrops on south-facing slopes, and the outcrops are dissected by joints and fractures.

The equigranular granite phase is generally medium-grained (0.2 to 0.5 centimeters) and massive (Figure 9). Major mineral components are 15 to 25% quartz, 45 to 55% plagioclase, less than 5% visible K-feldspar and 5 to 25% biotite. Similar rocks are found within the Idaho batholith near Robinson Bar and along the Payette River.

Average mineral percentages for the equigranular granite have been determined from thin sections and are given in Table 1. Appendix I gives the mineralogy and estimates for each thin section. The rock composition plots as granite to granodiorite (Figure 7). Alteration of primary minerals is abundant: biotite has characteristically gone to magnetite and chlorite, feldspars have been sericitized, and magnetite has further oxidized to hematite. Deformation is shown by strained grains of quartz and K-feldspar. Texture is massive and granular; myrmekite and lesser graphic intergrowths are found. Primary grains are 0.5 to 1.0 millimeter in length. BB-52 shows small (0.1 millimeter) grains of quartz and K-feldspar interstitial to phenocrysts of quartz, K-feldspar, and plagioclase, which make up 70% of the rock (Figure 10). These small grains represent either rapid crystallization of late-stage fluids or crystallization of eutectic melt.

Quartz Granite Porphyry

Quartz granite porphyry forms a stock along both sides of Basin Creek between the Salmon River and Hay Creek. This quartz porphyritic

Figure 7: Compositional plot of equigranular granite from the thesis area (circles) and the region (squares).

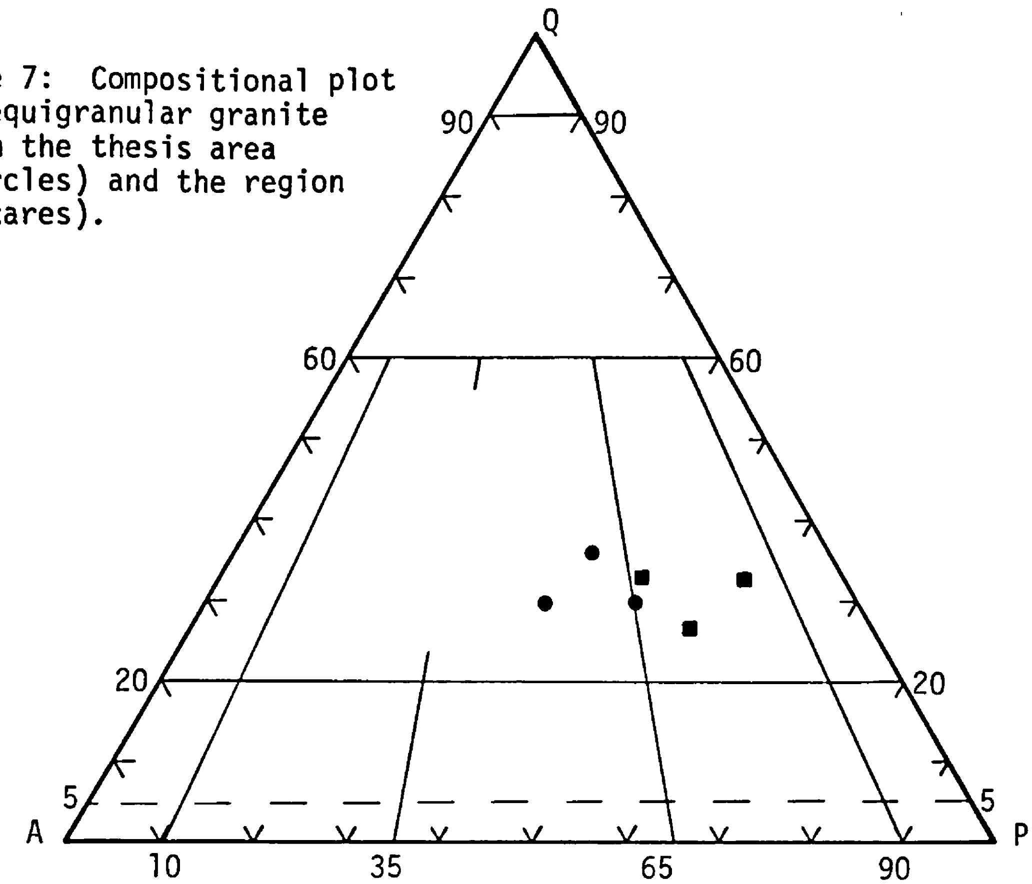

Figure 8: Compositional plot of quartz granite porphyry from the thesis area (circles) and the region (squares).

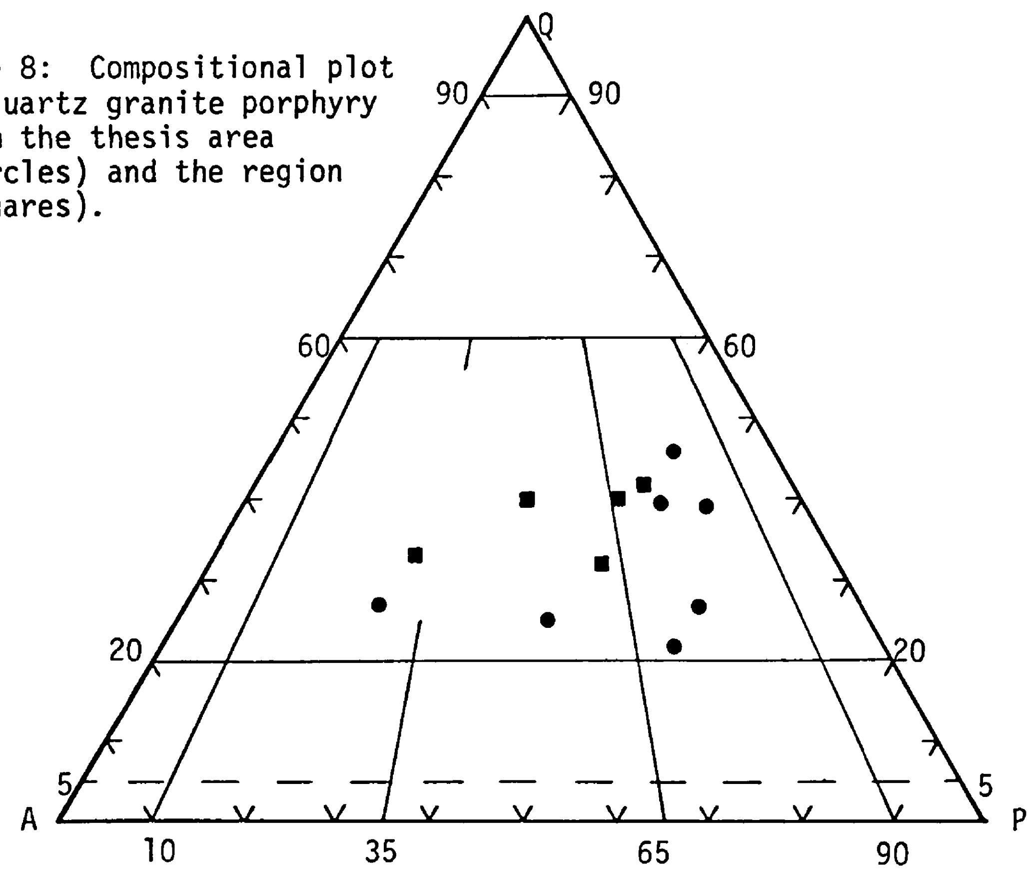

unit is exposed over 30% of the thesis area, and forms weathered outcrops on south-facing slopes. The poorly exposed unit crops out in less than 10% of its mapped area.

In hand specimen, the granite is medium-grained (0.5 cm) with subhedral gray quartz phenocrysts 1 cm across (Figure 11). The quartz phenocrysts are prominent on weathered surfaces. Overall mineralogy is 25% quartz, 45% plagioclase, 20% K-feldspar, and less than 10% biotite. The rock locally contains less than 5% K-feldspar megacrysts, appearing gradational to the K-feldspar porphyritic granite unit.

Average mineral percentages for the quartz granite porphyry have been determined from thin sections and are given in Table 1. Appendix I gives the mineralogy and percentages for each thin section. Figure 8 illustrates the compositional range: from granite to granodiorite. Alteration products are extensive and include brown clays, fine-grained white micas and carbonate after plagioclase, hematite after magnetite, leucoxene after sphene, and chlorite plus magnetite after biotite. Textures observed in thin section are fine-scale myrmekite (quartz intergrowths in plagioclase), sutured grain boundaries of quartz and K-feldspar, strained grains of quartz and K-feldspar, poikilitic K-feldspar megacrysts, and phenocrysts of quartz composed of many tiny grains to form single crystals up to 6 mm long (Figure 12).

K-Feldspar Porphyritic Granite

This unit is a potassium megacryst-bearing granite that covers 40% of the thesis area. The texturally distinctive unit crops out in two major areas of the thesis map: forming the eastern part of the map

Figure 9: Photograph of equigranular granite.

Figure 10: Photomicrograph of equigranular granite, BB-52, showing bimodal crystal size. Small grains are quartz and K-feldspar; large grains are quartz and plagioclase. 10x. Crossed polars.

Figure 11: Photograph of quartz granite porphyry

Figure 12: Photomicrograph of quartz granite porphyry, EBC-8, showing segmented quartz grains. Sutured quartz crystals form a single quartz megacryst. 10x. Crossed polars.

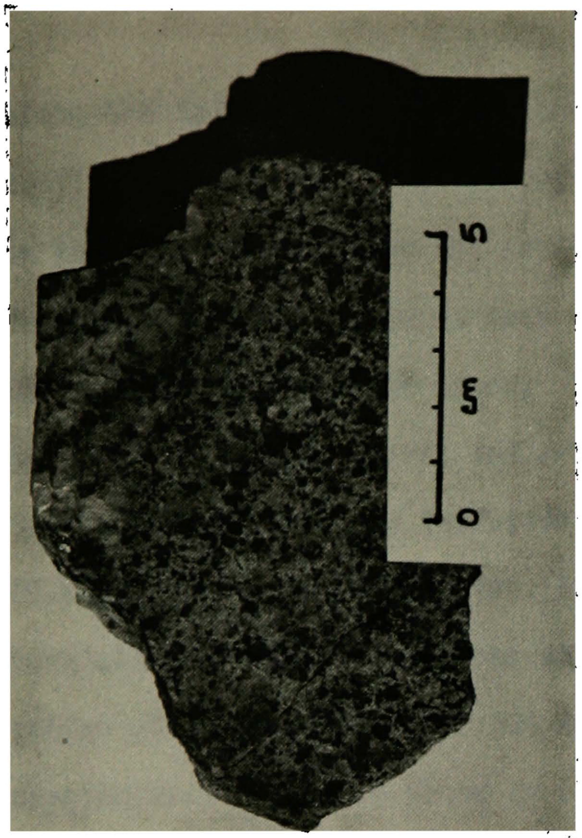
0 cm 5

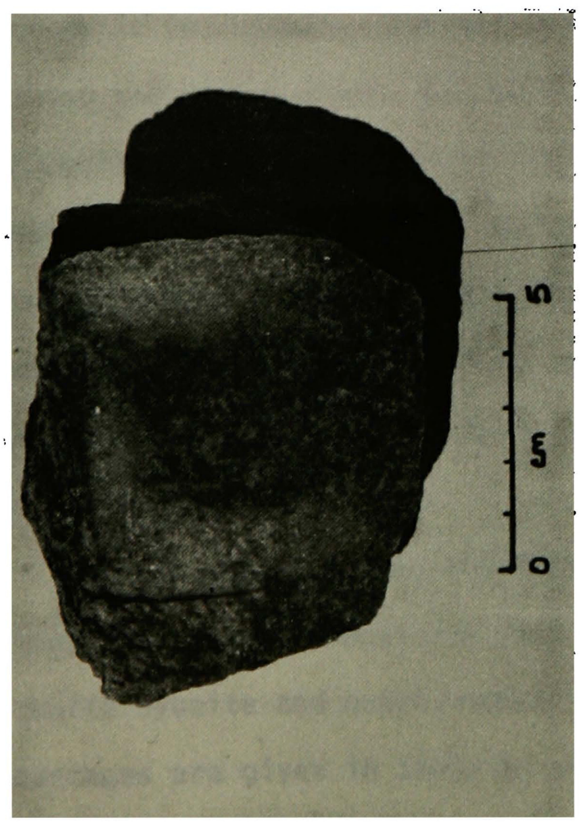
0 cm 5

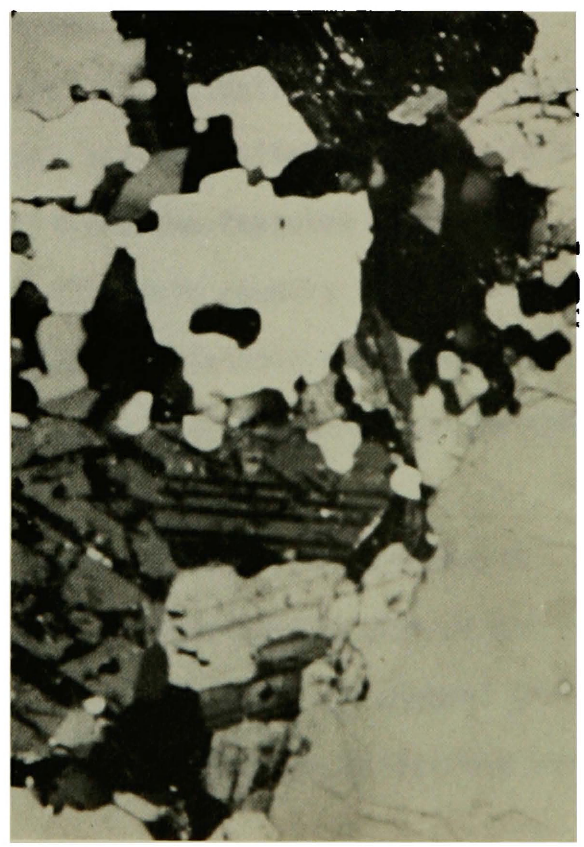

along the Salmon River, and at the Basin Creek-Little Basin Creek confluence. Like granites throughout central Idaho, exposure is poor in this unit on timbered and tree-covered slopes. The best outcrops are found along major drainages such as the Salmon River canyon between Basin Creek and American Creek. Outcrops are weathered, often to a granular texture of quartz and K-feldspar grains.

The porphyritic intrusive unit has a coarse-grained groundmass (0.5 to 1.0 cm) and is massive (Figure 13), except where megacrysts form clots or local lineations adjacent to shear zones. Typical composition of the rock is 20 to 30% clear to gray quartz, 40 to 60% white plagioclase, 10 to 20% white to pink K-feldspar, and 10% biotite. The K-feldspar megacrysts are up to 8 cm long and contain concentric zones of mafic inclusions. Between Lower Harden Creek and American Creek, along the Salmon River, the mafic content of the unit increases with the appearance of 2 to 4% hornblende. Small pods of foliated biotite-rich material also occur in the same area. These two features suggest contamination of the granitic magma by Paleozoic country rocks, or an earlier crystallized portion of the pluton. Paleozoic xenoliths found within the K-feldspar porphyritic granite will be discussed at the end of this unit description.

In thin section, K-feldspar porphyritic granite is found to have a range of composition from granite to granodiorite with minor quartz syenite and quartz monzonite (Figure 17). Average mineral percentages are given in Table 1, and Appendix I gives the mineralogy and percentages for each thin section.

Alteration is commonly observed in thin section; up to 50% of the plagioclase has broken down into sericite and minor coarse-grained muscovite, fine-grained carbonate and clays. Biotite has partially altered to chlorite, dusty magnetite and sphene. K-feldspar is commonly altered to sericite along microfractures.

Textures apparent in thin section are poikilitic K-feldspar megacrysts with quartz, plagioclase and biotite inclusions, braid and vein perthite (Heinrich, 1965) in orthoclase, and myrmekite fringing K-feldspar megacrysts (Figure 14). Deformation is typically observed within the intrusive unit: quartz crystals are composed of numerous optically disoriented grains with sutured boundaries, undulatory extinction in quartz, K-feldspar and plagioclase, bent biotite grains, and sutured grain boundaries between quartz, K-feldspar and plagioclase.

K-feldspar porphyritic granite is a texturally distinctive unit that is probably genetically related to quartz granite porphyry. The K-feldspar megacrysts appear to have grown late in the crystallization of the magma, as evidenced by their poikilitic nature. Aside from the presence of the megacrysts, the two textural units are identical. Some mechanism must have triggered the concentration of K-feldspar and subsequent formation of the megacrysts. The hornblende-bearing part of the unit is found only in the southeastern portion of the map area; it may be the result of assimilation of Paleozoic host rock or possibly a more mafic fringe of the unit. Numerous roof pendants are found locally between Lower Harden Creek and the Yankee Fork; the Idaho batholith-Paleozoic metasedimentary rock contact is exposed east of the Yankee Fork (Figure 3).

Figure 13: Photograph of K-feldspar porphyritic granite.

Figure 14: Photomicrograph of K-feldspar porphyritic granite, #11, showing a deformed orthoclase megacryst with some microcline (plaid) twins. Inclusions of quartz. 10x. Crossed polars.

Figure 15: Photograph of a typical outcrop of Idaho batholith in the Basin Creek area. Leucocratic granite above Lynch Creek. Hammer is 38 cm. long.

Figure 16: Photograph of leucocratic granite.

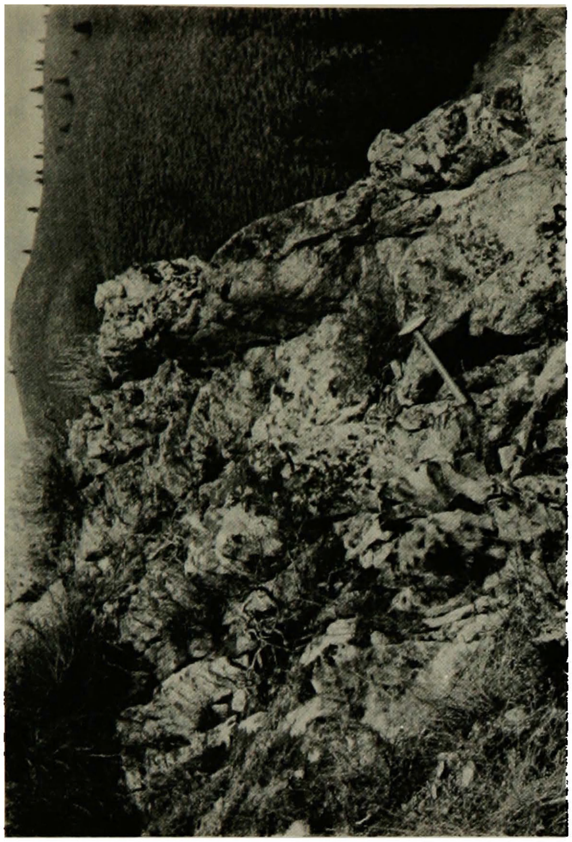

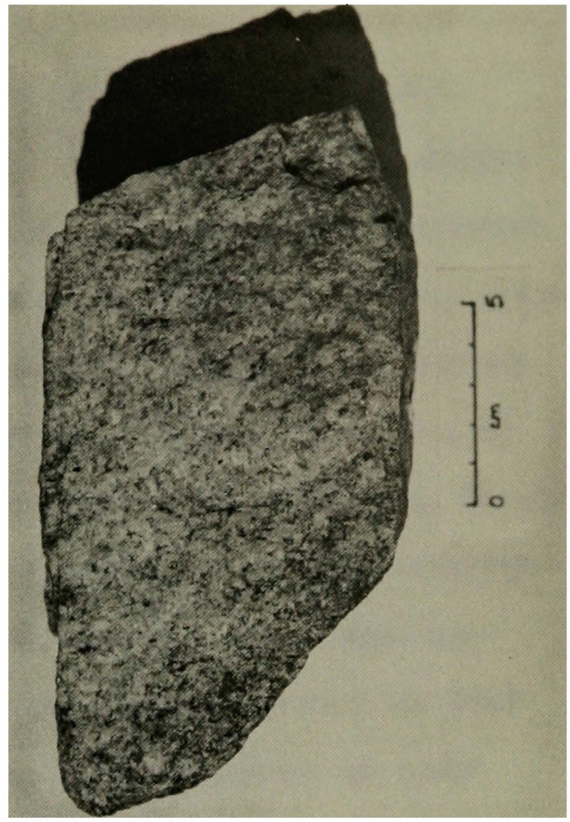
0 cm 5

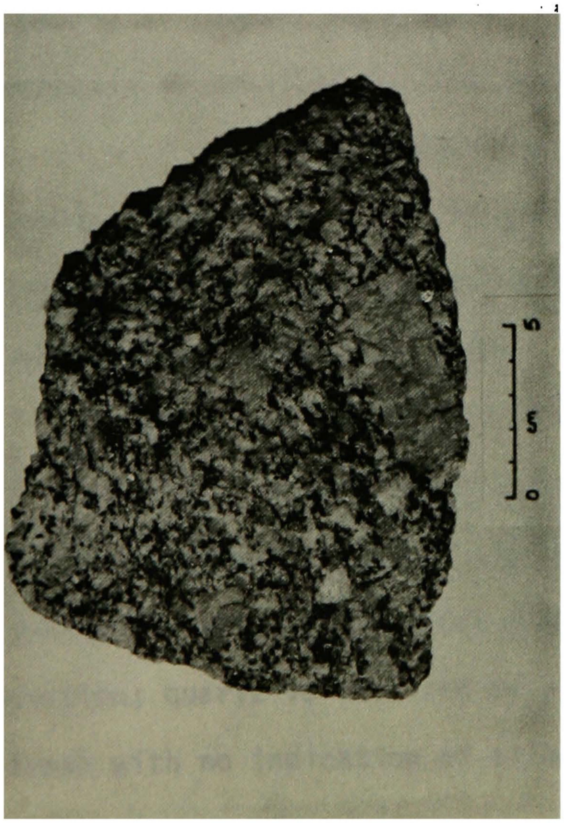
0 cm 5

<u>Paleozoic Xenoliths</u>. Two small occurrences of Paleozoic xenoliths are found in the thesis area. These xenoliths are related to country rock found several kilometers to the east along the Yankee Fork. The local batholithic host rock is the Pennsylvanian Wood River Formation, a thick metasedimentary package of limestones, quartzites and siltstones (Ross, 1937). One xenolith (100 by 15 by 20 meters) crops out just west of the Salmon River-Basin Creek confluence; Choate (1962) previously mapped the outcrop as basalt. The second xenolith (100 by 200 by 50 meters) is located in the upper end of American Creek. The stratigraphic location of the xenoliths within the Wood River Formation is not known as contact metamorphism by the Idaho batholith has obscured original sedimentary features and composition. Stoping of country rock during emplacement of the Idaho batholith is probably responsible for the xenoliths.

In hand specimen, the xenoliths are fine-grained. The American Creek occurrence is gray-black siltite with white quartzite interbeds. The Basin Creek outcrop is a black hornfels with abundant quartz veins cutting the rock.

A sample of the Basin Creek xenolith was examined in thin section. Minerals are quartz (45%) occurring in both the rock and veinlets, green hornblende (40%), plagioclase (15%, An_{43}), and accessory pyrite and sphene. The rock displays good hornfelsic texture in thin section; quartz is strained but grains are not oriented. The rock is fresh with no indication of alteration.

Figure 17: Compositional plot of K-feldspar porphyritic granite from the thesis area (circles) and the region (squares).

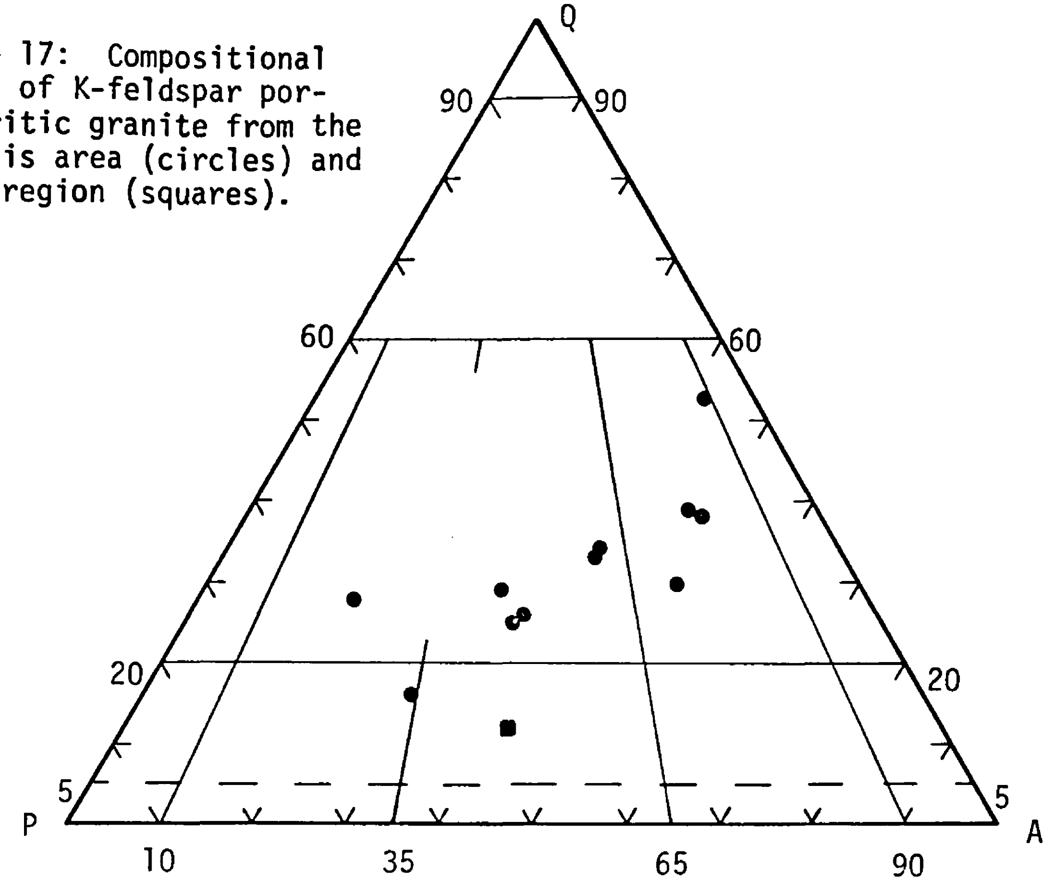

Figure 18: Compositional plot of leucocratic granite from the thesis area (circles) and the region (squares).

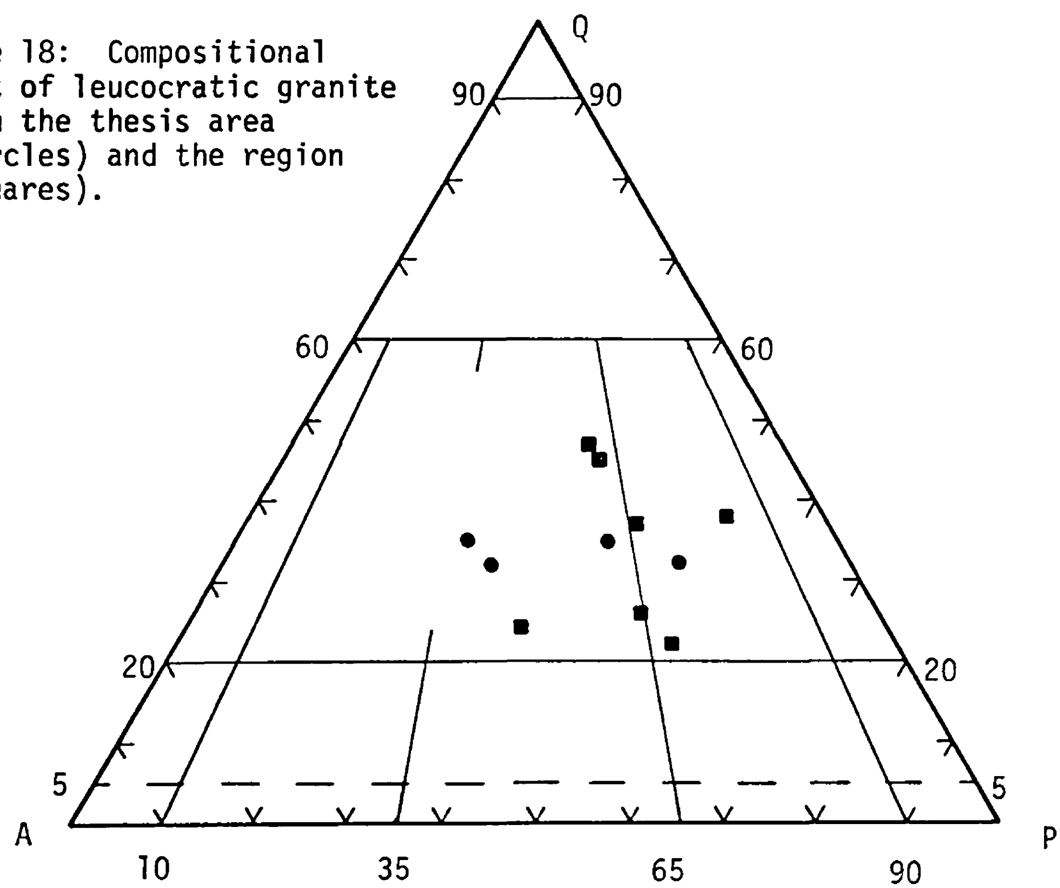

<u>Leucocratic Granite</u>

The leucocratic intrusive unit crops out over 7% of the thesis area; most outcrop is along a north-south trend parallel to East Basin Creek. The rock is generally fresh in appearance (probably because most outcrops are in drainages and are recently exposed; see Figure 15). This granitic unit is similar to rocks found locally elsewhere within the Idaho batholith (Reid, 1963).

In hand specimen, the leucocratic granite phase is equigranular, fine- to medium-grained (0.1 to 0.5 cm) and massive in outcrop (Figure 16). The mineralogical distinction between equigranular granite and leucocratic granite is the amount of biotite present: less than 5% for the leucocratic granite, and greater than 10% for the equigranular granite. Mineral assemblages observed in hand specimen are 25 to 40% quartz, 40 to 60% plagioclase, 10 to 20% K-feldspar, and less than 5% biotite.

In thin section, leucocratic granite ranges in composition from granite to granodiorite (Figure 18). Average mineral percentages are given in Table 1, and the mineralogy and percentages for each thin section are given in Appendix I. Textures observed in thin section indicate deformation of a partially cooled rock: sutured grain boundaries, undulose quartz, and segmented grains of optically discontinuous quartz. Crystallization textures include zoned plagioclase, poikilitic K-feldspar, embayed quartz, plagioclase and local biotite, interstitial myrmekite, and graphic intergrowths.

The leucocratic granite appears to crosscut all other Idaho batholith units in the study area. This relationship and the leucocratic nature of the rock indicates that it may be a late-stage differentiate of the batholith. This unit is similar in appearance to the White Cloud stock. The White Cloud stock and aplite and pegmatite dikes in the Idaho batholith have the same trace element chemistry (Bennett, 1973), suggesting a genetic relationship between the two late-stage differentiates. Other leucocratic rocks have been observed in the Idaho batholith and are also interpreted as late-stage differentiates of the batholith (Bennett, 1980).

Aplites and Pegmatites

Aplites and pegmatites are ubiquitous in the Idaho batholith but do not occur in the Challis volcanics. The felsic dikes range in thickness from one centimeter to greater than one meter and may display complex textures of multiple intrusions along the same fracture. Most outcrops are too small to locate on Plate I or Figure 5; only significant areas of outcrop were mapped. Sharp contacts with the host rock were observed everywhere.

In hand specimen, typical mineralogy includes pink K-feldspar, gray quartz, white plagioclase and clots of muscovite and/or biotite. Textures are sugary aplitic or coarse-grained pegmatitic (Figure 19).

In thin section, a "traverse" was taken across a pegmatitic dike-country rock contact. Adjacent to the country rock, the dike has a five-centimeter selvage of aplitic (less than one millimeter) material (EBC-41a). The dike coarsens inward to porphyritic and pegmatitic textures (EBC-41d). Mineralogy of the "traverse" is presented in Appendix I.

Figure 19: Photograph of a composite pegmatitic (white outer margins) and aplitic (gray inner zone) dike cutting K-feldspar porphyritic granite. Pencil is 15 cm. long.

Figure 20: Photograph of Tertiary rhyolite.

Figure 21: Photograph of Tertiary silicic dike.

Figure 22: Photomicrograph of uraninite (black) disseminated in bands of chalcedony from the Alta prospect, EBC-50. 10x. Plane light.

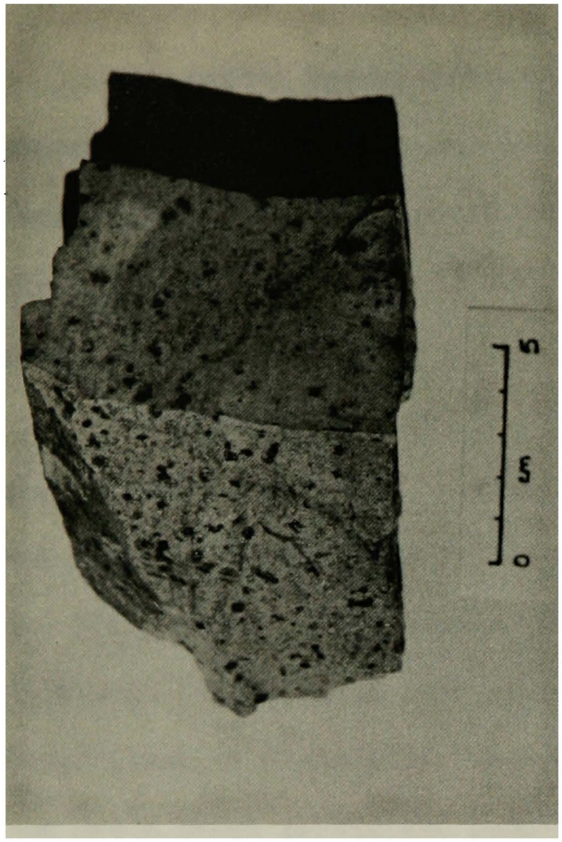
0
cm
5

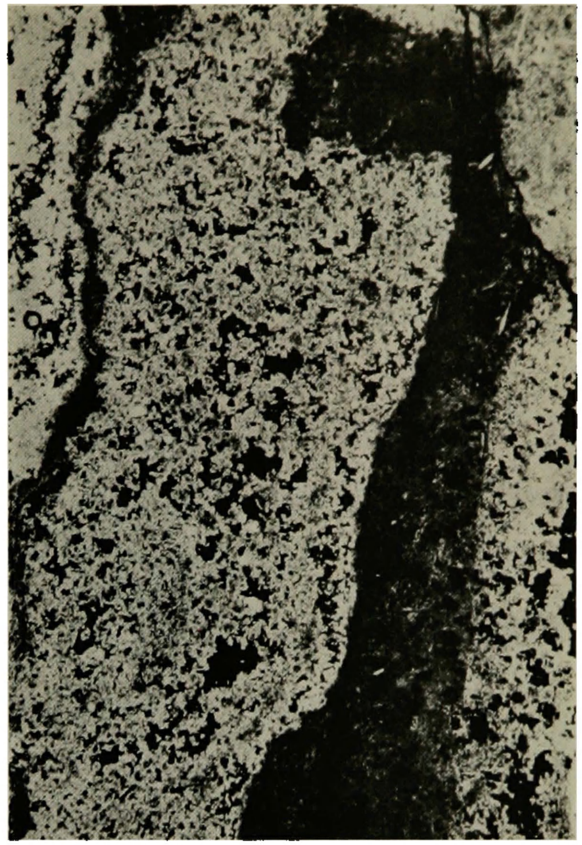

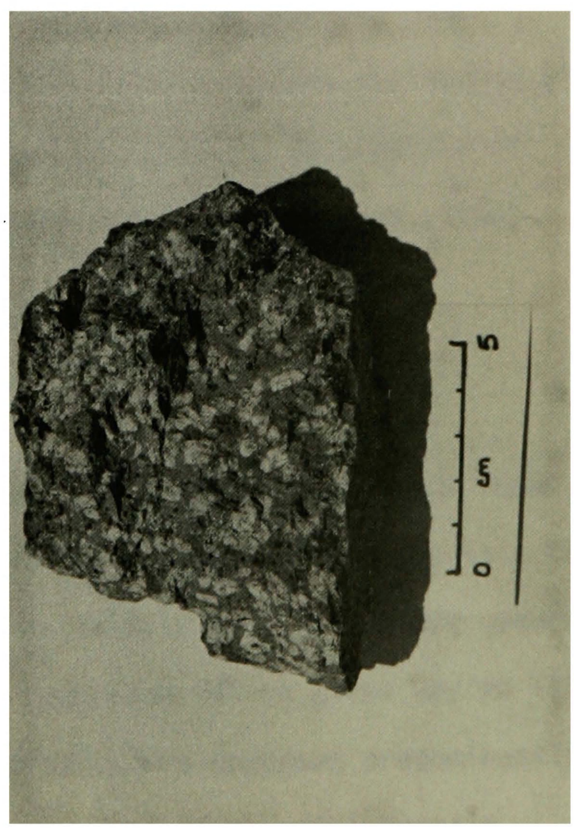
0
cm
5

No exotic pegmatitic minerals have been observed; accessory minerals include apatite and secondary muscovite. Fine-scale textures include myrmekite and graphic intergrowths. Deformation is seen in strained grains of quartz and K-feldspar and bent lamellae in plagioclase.

Aplites and pegmatites of the Basin Creek area do not occur in the leucocratic granite. Because no granitic dikes were observed near any contact of the leucocratic granite, age relations are uncertain. The dikes may be older than or the same age as the leucocratic granite. Cavanaugh (1979) notes that aplite and pegmatite dikes lace the White Cloud stock, a Cretaceous leucocratic granite south of the thesis area. The Basin Creek aplite and pegmatite dikes are of granitic composition that probably formed from fluids near eutectic composition. The pegmatitic dikes contained more volatiles which affected nucleation of grains and led to coarser crystals (Hyndman, 1972). Deformation of grains is common in pegmatites (Williams, Turner and Gilbert, 1954).

TERTIARY ROCKS

Arkose

Arkosic sediments which are derived from the Cretaceous Idaho batholith unconformably overlie the granitic rocks and are overlain in turn by the Challis volcanic pile. The arkosic sediments grade upward to carbonaceous shale and tuffaceous sandstone, which gives way to lithic tuff (Choate, 1962). The arkosic sediments are composed predominantly of subrounded quartz and feldspar grains with minor conglomeratic pebble and cobble lenses. The gray-white arkose is difficult to distinguish from the granitic rocks. The arkose contains abundant carbonaceous trash and secondary uranium mineralization. Arkosic sediments form the northeastern boundary of the map area; these sediments are the major uranium ore hosts in the Stanley area.

Volcanics - Undivided

In outcrop the Challis volcanics occur as dikes cutting and tuffs and flows overlying the Cretaceous granitic rocks. Many "basaltic" dikes observed in the field were too small to be shown on Plate I. The Challis volcanic pile unconformably overlies the batholith and conformably overlies the Tertiary arkose to the northeast of the thesis area. Within the study area most volcanic occurrences are small discontinuous dikes of fine-grained basalt. These rocks usually are gray-green with less than 5% phenocrysts of plagioclase and pyroxene.

In thin section, one specimen (BB-40) contains 35% plagioclase (An_{54}), 30% chlorite, greater than 30% sericite, and 5% magnetite. Accessory minerals include carbonate and resorbed grains of quartz. Chlorite has replaced ferromagnesian minerals (pyroxene?) and is characteristically rimmed by magnetite. Some apparently primary magnetite is also found in the rock. Sericite and carbonate have formed from the breakdown of feldspar. The rock is completely crystalline, with 12% phenocrysts of plagioclase and minor quartz and magnetite. The resorbed quartz is out of equilibrium with the basaltic rock; minor resorption is also observed in plagioclase and ferromagnesian grains.

Several blocks of Tertiary volcanics are found in the Idaho batholith along Basin Creek between Hay Creek and Short Creek. These blocks appear to be normal fault-bounded and may have dropped from structurally higher levels near the erosional top of the batholith.

Rhyolite

Porphyritic rhyolite dikes and plugs intruded the Challis volcanics and the underlying Idaho batholith. Rhyolite was also extruded but is found predominantly outside the thesis area. The rhyolite bodies crop out prominently and are easily traced both on aerial photographs and on the ground. The hypabyssal rhyolite forms a northeast-trending dike swarm in the Potato Mountain area. Age of the rhyolite is uncertain; it appears to be younger than most of the Challis volcanism in the region. The northeast-trending rhyolite dikes may be related to the gray quartz latite of the Idaho porphyry belt (Olson, 1968).

In hand specimen, the rhyolite is porphyritic (Figure 20) with phenocrysts of clear to gray quartz (1 to 3 mm), chalky white to pink feldspars (2 to 5 mm), and green-black biotite (1 mm). The gray-green aphanitic groundmass makes up 75 to 90% of the rock. Some quartz grains are euhedral crystals of beta-quartz.

In thin section, rhyolite consists of 10 to 25% phenocrysts of quartz, plagioclase, K-feldspar, biotite and minor hornblende. Quartz grains are euhedral but embayed on several sides. No deformation is seen within individual quartz grains which occur singly or in clusters as glomerocrysts. Quartz comprises approximately 50% of the phenocryst component. Plagioclase makes up to 30% of the phenocrysts. Plagioclase has albite twins and forms glomerocrysts with other plagioclase grains. There is minor synneusis texture where the plagioclase grains join and grow rims (Vance, 1969). Almost all observed plagioclase crystals are anhedral and well altered to fine-grained white micas. K-feldspar (15 to 30% of the phenocryst component) forms large altered phenocrysts which have rounded edges and abundant microfractures along which alteration is pervasive. The most abundant alteration minerals within K-feldspar crystals are fine-grained sericite and carbonate. Biotite forms 1% of the phenocrysts, and hornblende is rarely found as an accessory phenocryst. Both brown biotite and hornblende have been largely replaced by chlorite, magnetite, hematite, and calcite. The groundmass is composed of fine-grained K-feldspar (10 to 30%), quartz (15-20%), plagioclase (5 to 20%), disseminated magnetite (2%) and chlorite (10%) with abundant clay and devitrified brown glass. Appendix I gives the mineral percentages.

The embayed alpha-quartz paramorphs after beta-quartz indicate that quartz crystals were formed at high pressures and temperatures; magmatic corrosion of the crystals resulted from a drop in pressure within the magma, making quartz unstable in the melt (Whitney, 1975a). The resorption of quartz within the magma results from changing conditions within the magma and/or from a changing magma composition.

Tertiary rhyolite is a hypabyssal, porphyritic rock that formed some crystals (phenocrysts) at depth. The presence of tiny crystals and glass within the groundmass indicates that little time was available for crystallization between emplacement and solidification of rhyolitic magma.

Silicic Dikes

Silicic dikes crop out west of Basin Creek along several ridges. The dikes are one to three meters wide and discontinuous on the surface. Outcrops are pervasively jointed and fractured so that hand specimens are no longer than 15 cm. The dikes cut only the Cretaceous granitic units in the Basin Creek area; age relationships with the Challis volcanics are uncertain. To the north of the thesis area, near Knapp Lakes, similar dikes cut an Eocene pluton (David Obolewicz, 1979, personal communication). Although these dikes have no apparent trend within the thesis area, they may be related to the Tertiary dikes of the Idaho porphyry belt (Olson, 1968). Olson described similar rhyolite dikes northwest of Stanley that are aphanitic with local impregnations of pyrite.

The silicic dike rock is buff white and weathers to tan, pink or pale green. The rock is resistant to weathering and forms fractured outcrops along ridge crests. Texture is porphyritic with an aphanitic groundmass (Figure 21). Phenocrysts of quartz, K-feldspar, and pyrite are few (1 to 2%); the only visible mafic minerals are iron sulfides and oxides. Pyrite has commonly weathered out leaving behind a "limonitic" boxwork in cubic holes.

In thin section, the porphyritic rock has phenocrysts of anhedral quartz (0 to 5%), K-feldspar (0 to 3%), and pyrite cubes ($<$1%). The groundmass is very fine-grained and composed of quartz (40 to 60%), K-feldspar (25 to 50%), plagioclase laths (0 to 30%), and fine-grained white mica (5 to 15%). Appendix I gives mineral percentages for each thin section. Groundmass textures include spherulites of radial intergrowths of quartz and K-feldspar and graphic texture where quartz and K-feldspar are intergrown. Graphic quartz, in many cases, is optically continuous around quartz phenocrysts. Alteration of the feldspars and pyrite is extensive; typical alteration products are sericite, clay, carbonate, and iron oxides.

QUATERNARY DEPOSITS

In the Basin Creek area Quaternary deposits are predominantly recent alluvium with minor glacial deposits. The recent alluvium includes fluvial and flood-plain sands, silts, and gravels, slope wash, and some glacial outwash. Glacial deposits are abundant in the headwaters of Basin Creek; a poorly sorted terminal moraine fills the Basin Creek valley at the northern edge of the thesis area. Williams (1961) has mapped and described the glacial deposits of Stanley Basin.

CHAPTER IV

CHEMISTRY

Chemical analyses of the granitic rocks within the Basin Creek area have been studied to determine if there are any genetic affinities within the rocks. Numerous two and three component variation diagrams were drawn. Simple variation diagrams illustrate the chemical variation within the rock suite. Complex binary diagrams attempt to show differentiation trends within a crystallizing magma, with the inherent assumption that the observed variation is controlled by differentiation. CIPW norms were calculated from chemical analyses and were compared to experimentally determined phase diagrams. Phase diagrams give a theoretical basis for comparison of real rocks. An important point in the following discussion is that only eleven analyses are used to define a curve; many more analyses are required to create a statistically valid curve.

ROCK CHEMISTRY

Major-oxide chemistry of eleven representative rocks is shown in Table 2. Three average igneous rock analyses (Hyndman, manuscript) are given for comparison. Immediately obvious is the silica range: 65 to 77%. Because of the large percentage of SiO_2, the remaining major oxides are in negative correlation and are controlled by a 100% total. Chemical variation diagrams are constructed assuming that one magma series is being examined.

Table 2. Chemical compositions (oxides, weight %), and CIPW norms of selected rocks from the Basin Creek area, Idaho.

	1	2	3	4	5	6	7	8	9	10	11	12	13	14
SiO_2	75.51	66.99	68.53	69.71	68.33	70.64	65.59	71.29	72.36	73.82	77.07	72.04	69.51	66.80
TiO_2	0.14	0.33	0.50	0.49	0.49	0.57	0.75	0.26	0.19	0.16	0.06	0.30	0.51	0.54
Al_2O_3	13.51	14.90	16.23	14.89	14.59	13.90	14.79	13.94	13.12	11.97	12.43	14.42	14.76	15.99
Fe_2O_3	0.48	0.98	0.95	1.18	1.52	1.75	1.59	0.65	0.66	0.55	0.06	1.22	1.26	1.52
FeO	0.75	1.05	1.80	1.55	1.25	1.65	2.40	1.25	0.75	1.05	0.60	1.68	2.15	2.87
MnO	0.02	0.07	0.04	0.04	0.04	0.05	0.06	0.03	0.02	0.04	0.01	0.05	0.08	0.08
MgO	0.22	0.61	1.01	0.90	0.88	1.21	1.80	0.51	0.26	0.36	0.10	0.71	1.11	1.80
CaO	0.65	1.78	2.89	2.91	2.83	2.84	3.83	1.95	1.18	1.68	0.07	1.82	2.55	3.92
Na_2O	3.60	3.93	3.77	3.56	3.37	3.58	3.48	3.70	3.13	1.65	3.43	3.69	3.51	3.77
K_2O	4.36	3.99	3.16	3.19	3.98	3.71	3.81	4.47	5.46	5.67	4.59	4.12	4.14	2.79
P_2O_5	0.05	0.15	0.21	0.20	0.20	0.22	0.31	0.10	0.06	0.05	0.04	0.12	0.19	0.18
Total	99,29	94,78	99,09	98.62	97,48	100.12	98,41	98.15	97.19	97.00	98.46	100.17	99.77	100.26

Table 2. Continued.

	1	2	3	4	5	6	7	8	9	10	11	12	13	14
Q	35.96	24.29	26.66	29.32	26.61	28.43	20.66	27.56	30.28	37.96	38.94	29.46	25.72	22.18
C	1.82	1.28	1.91	0.82	0.12				0.07	0.20	1.80	0.90	0.37	0.12
or	25.76	23.58	18.67	18.85	23.52	21.92	22.51	26.41	32.26	33.50	27.12	24.35	24.46	16.49
ab	30.46	33.25	31.90	30.12	28.51	30.29	29.44	31.31	26.48	13.96	29.02	31.22	29.70	31.90
an	2.86	7.75	12.83	13.00	12.60	10.90	13.48	8.23	5.42	7.97	0.06	8.17	11.28	18.15
di						1.05	1.92	0.31						
he						0.22	0.73	0.29						
en	0.55	1.52	2.52	2.24	2.19	2.52	3.59	1.13	0.65	0.90	0.25	1.77	2.76	4.48
fs	0.79	0.70	1.77	1.14	0.30	0.62	1.58	1.23	0.56	1.28	0.97	1.67	2.21	3.27
mt	0.70	1.42	1.38	1.71	2.20	2.54	2.31	0.94	0.96	0.80	0.09	1.77	1.83	2.20
il	0.27	0.63	0.95	0.93	0.93	1.08	1.42	0.49	0.36	0.30	0.11	0.57	0.97	1.03
ap	0.12	0.36	0.50	0.47	0.47	0.52	0.73	0.24	0.14	0.12	0.09	0.28	0.45	0.43
Total	99.29	94.78	99.09	98.60	97.45	100.09	98.37	98.14	97.18	96.99	98.45	100.16	99.75	100.25

Table 2. Continued.

Rock samples:

1 Equigranular granite -- BB-71.

2 Quartz granite porphyry -- BB-70.

3 Quartz granite porphyry -- BB-73.

4 K-feldspar porphyritic granite -- EBC-15.

5 K-feldspar porphyritic granite -- EBC-47.

6 K-feldspar porphyritic granite -- EBC-48.

7 Hornblende-bearing K-feldspar porphyritic granite -- EBC-49.

8 Leucocratic granite -- EBC-52.

9 Leucocratic granite -- EBC-53.

10 Rhyolite dike -- EBC-51.

11 Silicic dike -- EBC-54.

12 Average composition of alkali-feldspar granite (Hyndman, manuscript).

13 Average composition of granite (Hyndman, manuscript).

14 Average composition of granodiorite (Hyndman, manuscript).

Analyst: Technical Service Laboratories, Mississauga, Ontario, Canada.

The chemistry of an igneous rock is closely related to the chemistry of the magma from which it crystallized. However, coarse-grained plutonic rocks may not represent the chemistry of the magmatic liquid from which they cooled (Wilcox, 1979). Crystal settling or filter-press action may shift the original composition of the magma so that the rock chemistry for the Basin Creek area may or may not be the same as the original magma.

Silica Variation Diagrams

Figure 23 shows each of the major oxides plotted against SiO_2. Linear trends are found in each oxide diagram with an apparently systematic relationship between each oxide and silica. Silica variation (Harker) diagrams are often used with the assumption that within the course of evolution of a magma series there is always a continuous increase in silica content. This is not always a valid assumption (Charmichael, Turner, and Verhoogen, 1974, p. 46).

Straight line variation of chemistry within each diagram is commonly interpreted as a co-magmatic rock suite (Wilcox, 1979). However, the coarse-grained rock suite may not represent a continuous liquid line of descent, even if the rocks are all derived from a common parent magma. Coarse-grained plutonic rocks tend to show some evidence of crystal accumulation and slow cooling resulting from deep emplacement; this allows the remaining liquid to change its composition in unanticipated ways.

Binary Diagrams

Calculations used to create other binary diagrams attempt to

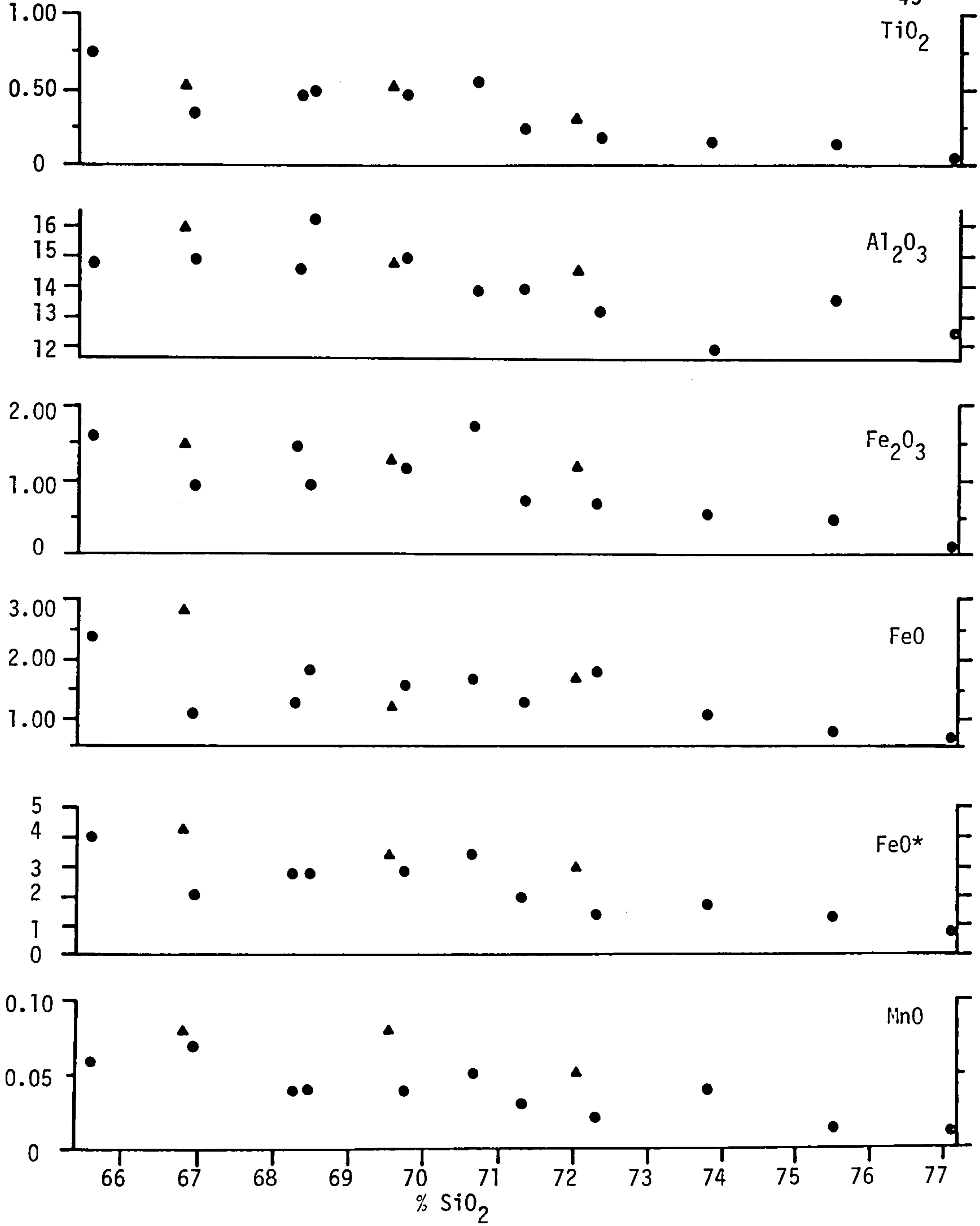

Figure 23: Silica variation diagrams of Basin Creek rocks (circles) and average rock types (triangles; Hyndman, manuscript).

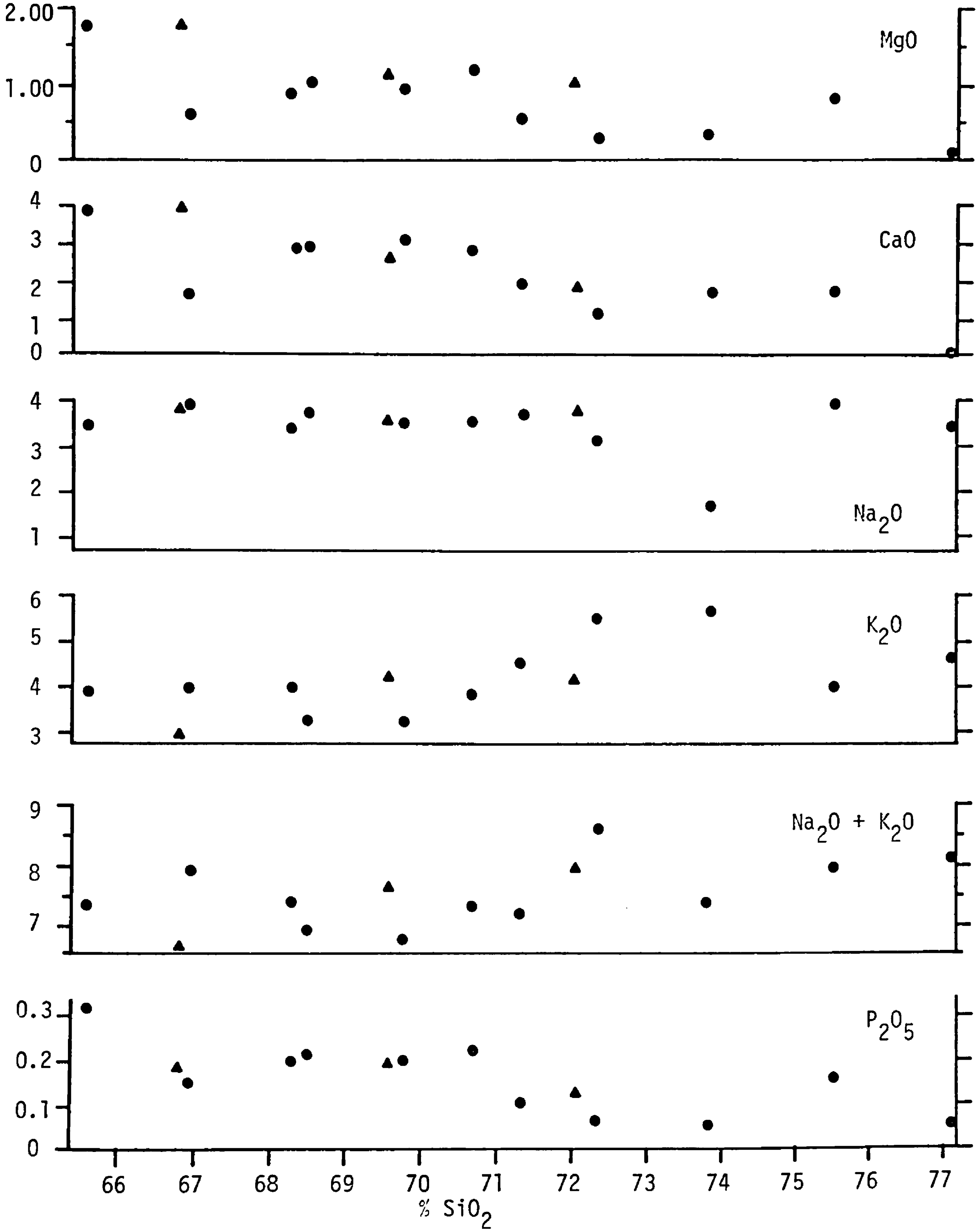

Figure 23: Continued.

show differentiation within a crystallizing magma. The chemical variation is assumed to be controlled by magmatic differentiation. Figure 24 shows four binary diagrams which illustrate broad, ill-defined trends. The abscissas of these diagrams represent equations. The differentiation index (Thornton and Tuttle, 1960) is the sum of the weight percents of normative quartz, orthoclase, albite, nepheline, leucite, and kalsilite, but no anorthite. Kuno's solidification index is $(100MgO)/(MgO + FeO + Fe_2O_3 + Na_2O + K_2O)$ (Cox, Bell, and Pankhurst, 1979). The Larsen index is $(1/3)SiO_2 + K_2O - (FeO + MgO + CaO)$ (Larsen, 1938). Magmatic differentiation probably occurred within the Atlanta lobe of the Idaho batholith but is not demonstrated by the limited group of chemical analyses from the Basin Creek area.

Ternary Diagrams

Normalized three-component systems are plotted to observe the mutual relations of the components. The CaO-K_2O-Na_2O diagram (Figure 25) does not display an obvious pattern; on closer inspection, the K-feldspar porphyritic granite samples cluster together with subequal amounts of each component. All other Basin Creek rocks contain distinctly less CaO but show no pattern to their arrangement. An AFM diagram (Figure 26) shows the expected trend of alkali enrichment. The Skaergaard iron-enrichment trend and Mount Lassen calc-alkalic trend are shown for comparison.

CIPW NORM CLASSIFICATION

Chemical analyses have been recalculated to a standard set of "normative" minerals (Cross and others, 1902; Hutchinson, 1974;

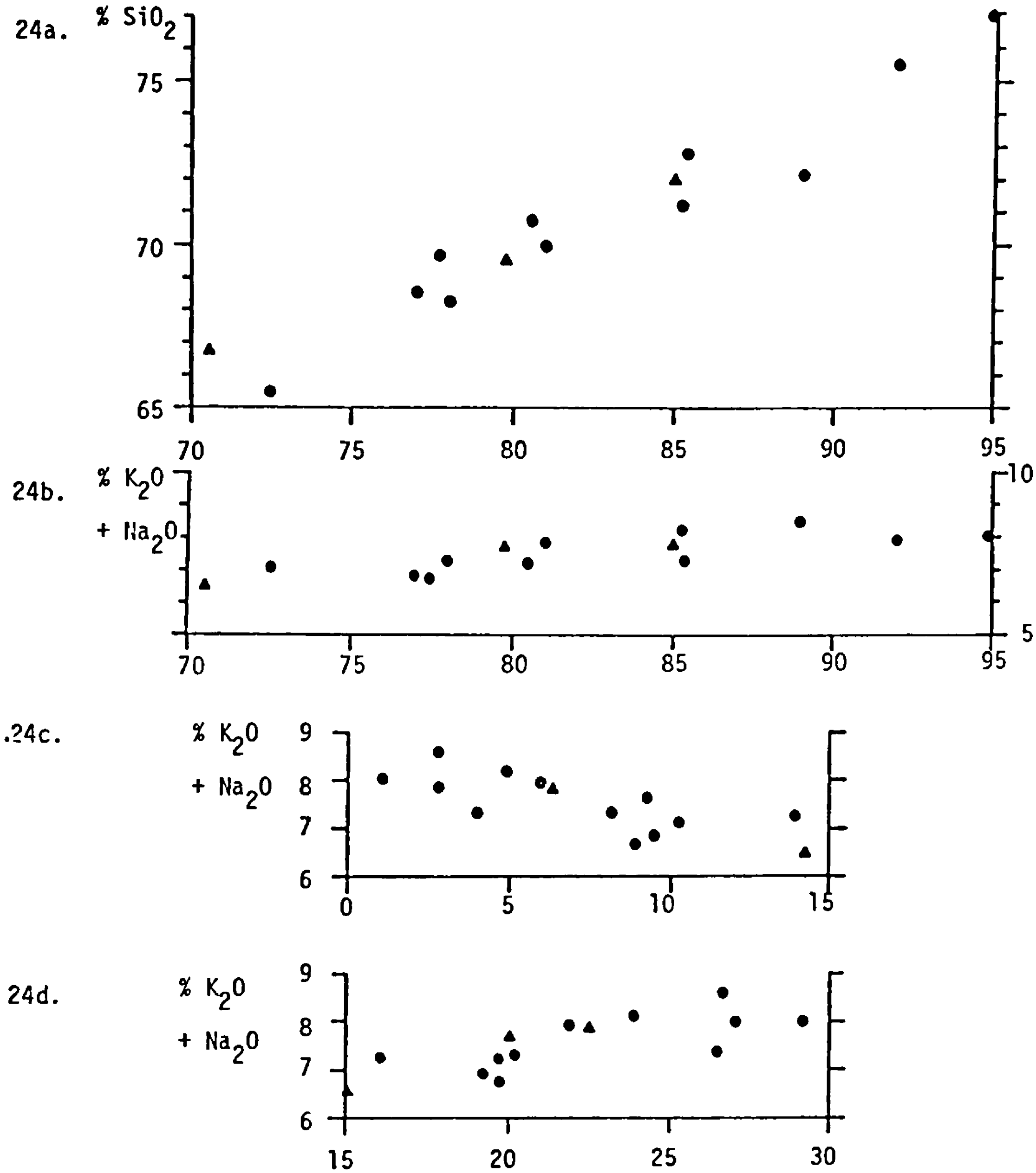

Figure 24: Binary variation diagrams.

a: Silica (%) vs. differentiation index.
b: Alkalis (%) vs. differentiation index.
c: Alkalis (%) vs. Kuno's solidification index.
d: Alkalis (%) vs. Larsen index.

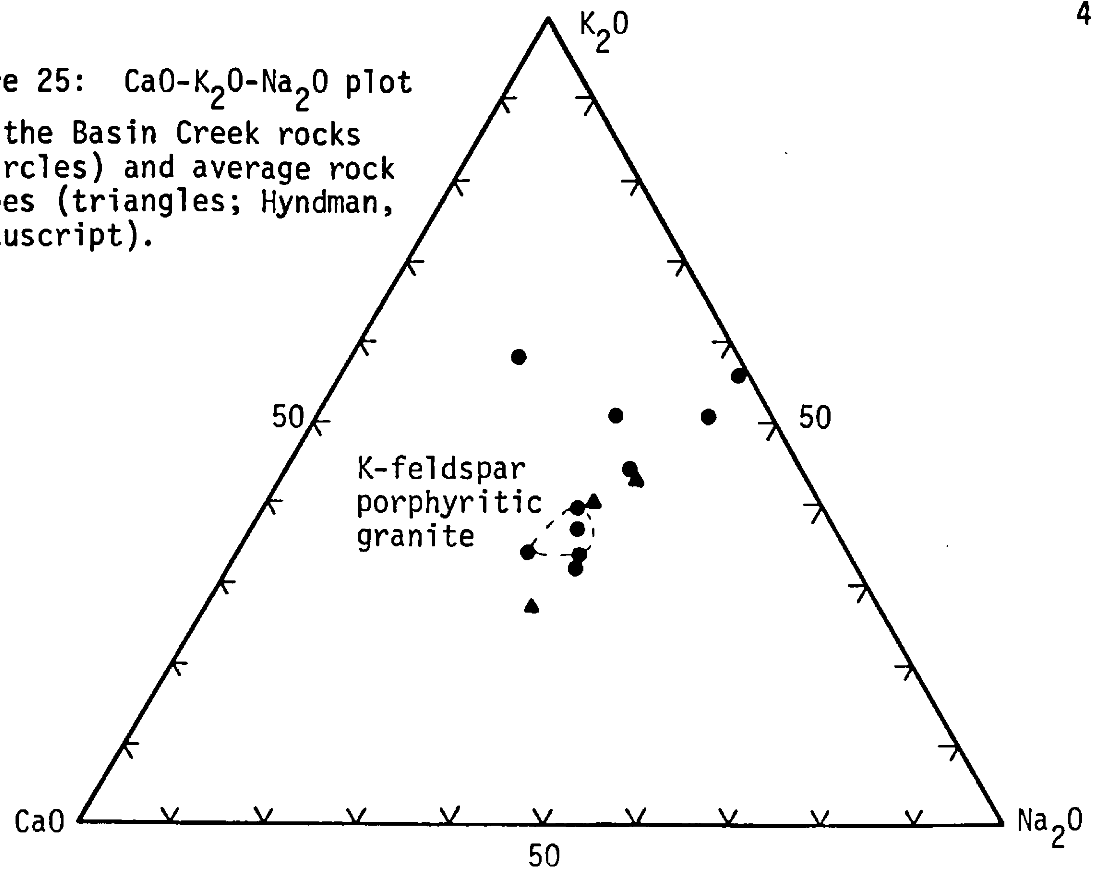

Figure 25: $CaO-K_2O-Na_2O$ plot of the Basin Creek rocks (circles) and average rock types (triangles; Hyndman, manuscript).

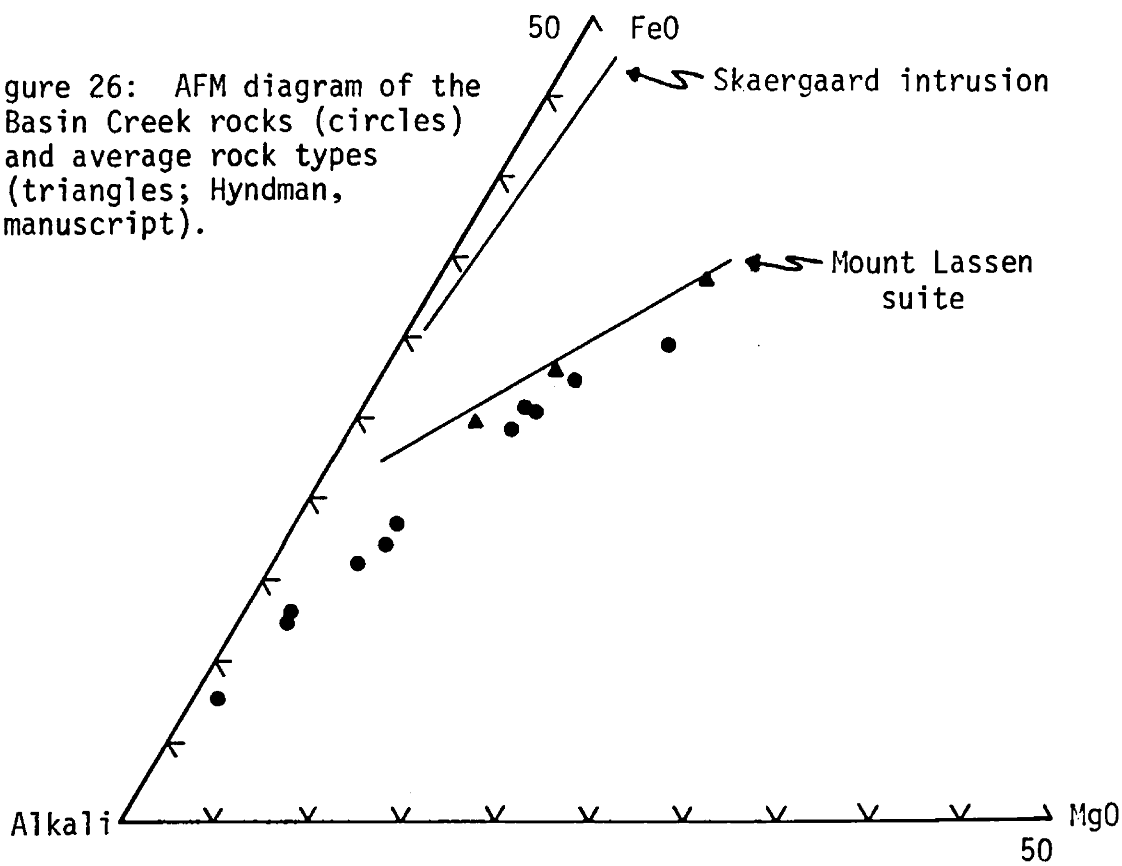

Figure 26: AFM diagram of the Basin Creek rocks (circles) and average rock types (triangles; Hyndman, manuscript).

Johannsen, 1939). This classification is generally used for volcanic rocks but shall be used for comparative purposes here. Results are shown on Table 2. Plots of normative minerals with experimentally derived cotectics show relationships between experimental data and the Basin Creek rocks. A normative feldspar ternary diagram (Figure 27) shows that only those rocks greater than 72% SiO_2 plot in the potassium-feldspar-first field. All other rocks plot in the plagioclase-first field, as confirmed by petrographic observations. A normative plot of Q-Ab-Or shows the effect of quartz added to an experimental crystallization system (Figure 28). Most Basin Creek rocks are predicted to crystallize quartz before alkali feldspar. The Basin Creek granitic suite is found to be representative of the Idaho batholith (Figure 29).

EVOLUTION OF THE GRANITE

Petrographic Criteria

The apparent order of initial crystallization of rock-forming minerals has been determined for the Basin Creek granitic rocks: plagioclase, quartz then K-feldspar, or K-feldspar then quartz, and finally biotite. I could not determine an absolute order of crystallization from the relative relationships. This sequence was determined from thin sections based on euhedral crystals, crystal size, composition of inclusions, and interstitial crystals. The Basin Creek granites are subsolvus granites (Tuttle and Bowen, 1958) since plagioclase and K-feldspar occur as separate grains. Lack of muscovite indicates that the granites either did not crystallize at sufficient depth or did not

Figure 27: Normative feldspar ternary diagram of Basin Creek rocks (circles) and average rock types (triangles; Hyndman, manuscript), Cotectics from Winkler (1979, p. 303, 304).

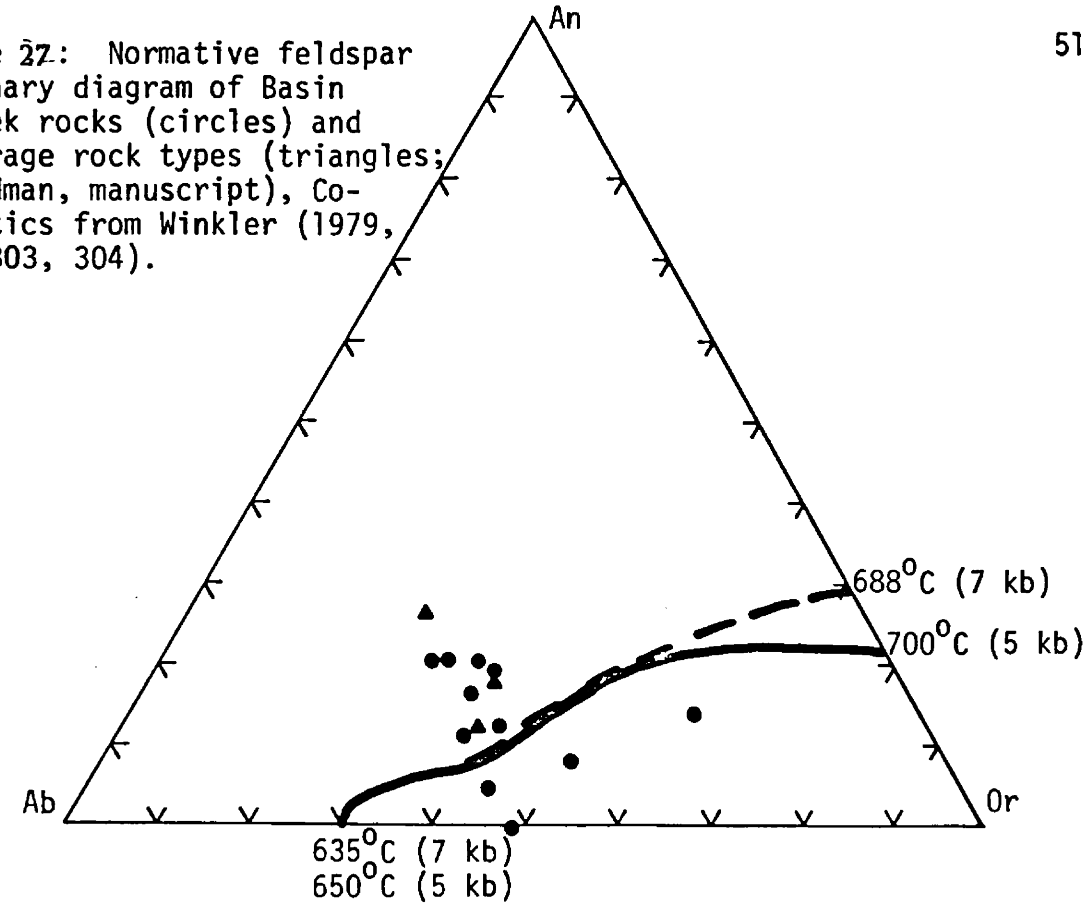

Figure 28: Normative Q-Ab-Or ternary diagram of Basin Creek rocks (circles) and average rock types (triangles; Hyndman, manuscript). Cotectics from Winkler (1979, p. 303, 304).

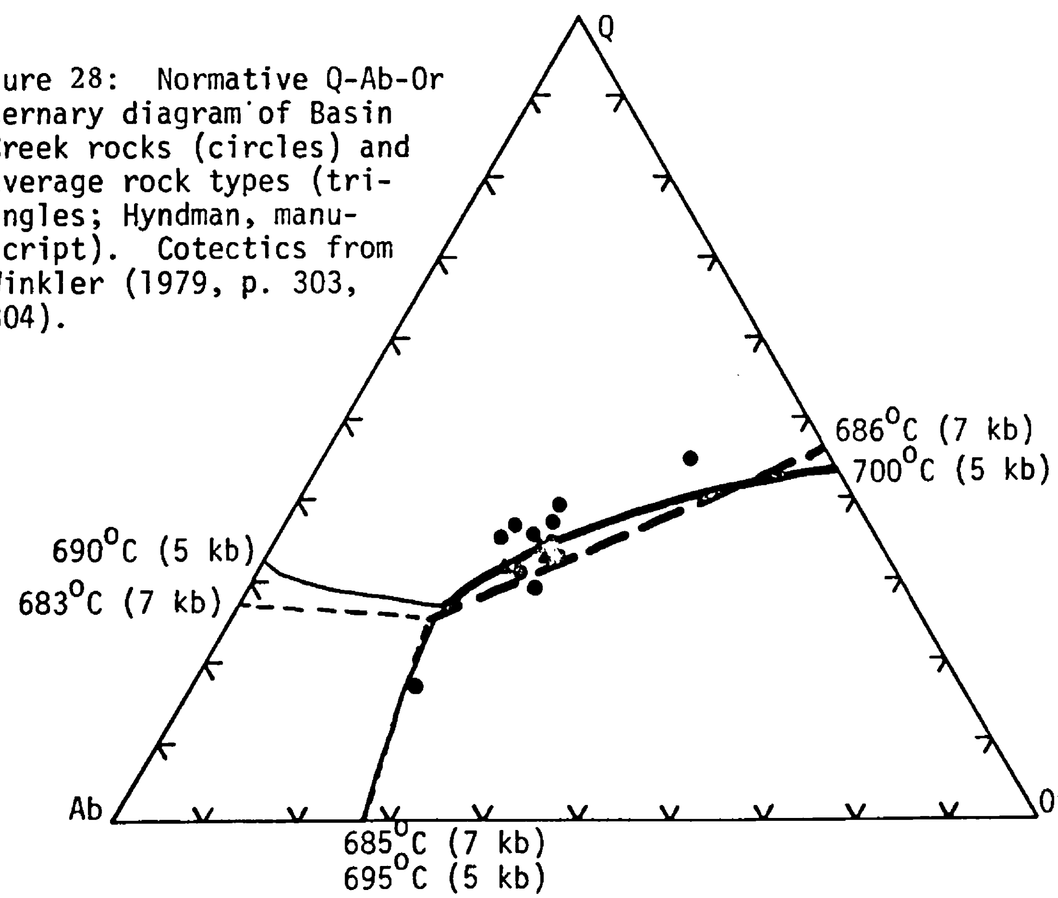

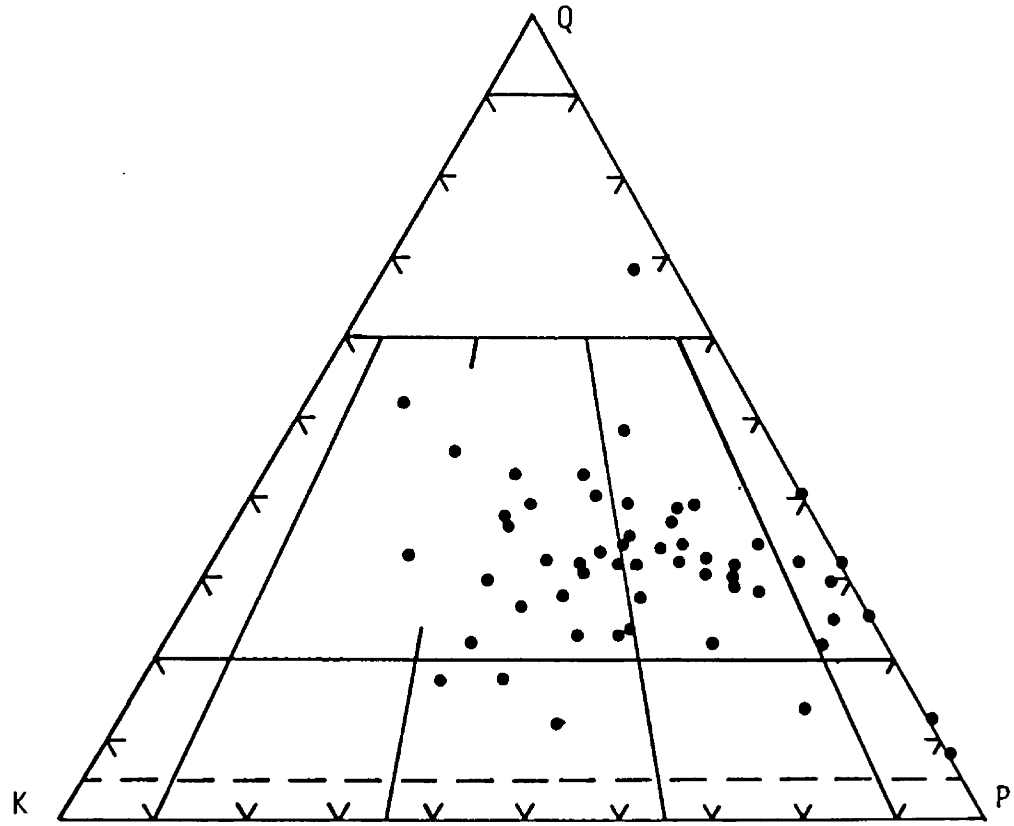

Figure 29: Modal analyses from the Idaho batholith (after Ross, 1963, p. C88).

contain the correct chemistry for muscovite formation. Locally, concentrically zoned plagioclase crystals appear in the granites; the zoning is the result of changing plagioclase composition in the magma. The change of plagioclase composition within the melt must be subtle as only a few zoned crystals are seen. K-feldspar megacrysts are generally rimmed by concentric rings of quartz, plagioclase and biotite inclusions. The megacrysts may have grown as late-stage magmatic crystals from a eutectic melt or by remobilization related to pegmatitic fluids. Some of the granitic rocks show evidence of late-stage rapid cooling because of a bimodal grain size where most of the rock is coarse-grained and equigranular but the groundmass is fine-grained and composed of equigranular quartz and K-feldspar.

Post crystallization textures within the Basin Creek granites show deformation and exsolution. K-feldspar is perthitic, with albite exsolving out of K-feldspar crystal structures as the rock cools. Myrmekite of quartz intergrowths in plagioclase form adjacent to K-feldspar crystals as a result of metasomatism or possibly exsolution (Parker, 1970). Alteration of deuteric/hydrothermal and/or surficial origin has formed chlorite and magnetite from biotite, and sericite, carbonate and clay from feldspars. Deformation of quartz grains in many rocks is shown by undulose extinction and segmented grains. K-feldspar crystallized as orthoclase (monoclinic) but later strain has deformed the crystal lattices into the lower symmetry of triclinic microcline.

Experimental Criteria

The Idaho batholith is a composite of plutons which show little, if any, vesiculation, a coarse grain size, and contemporaneous pegmatites (Hyndman, 1972, p. 136, 140-141). These mesozonal characteristics form at crustal depths of 7 to 13 kilometers with pressures of 2 to 4 kilobars. The magmas forming the plutons were undersaturated in water. When crystallization was almost complete, a water-saturated phase (pegmatites) was developed within the magmas (Whitney, 1975a). The composition and amount of the water-saturated phase generated by crystallization depends on the volatile content, lithostatic pressure, and degree of equilibrium in the magma. This phase may have been retained within the crystallizing pluton or expulsed to form pegmatitic dikes within previously crystallized plutons. The water-saturated phases of individual plutons are important in the concentration of volatiles and other elements, including uranium and thorium, that do not fit easily into the crystal lattices of major minerals: quartz, plagioclase, K-feldspar, and biotite, found within the granites.

Data on closed-system isobaric experiments on batholith crystallization give the expected order of crystallization within a granitic magma at various water contents (Wyllie and others, 1976). Quartz and plagioclase are anticipated liquidus minerals (Stern and others, 1975) for a water-undersaturated magma.

Given the observed crystallization sequence and a reasonable 2 kbar pressure for mesozonal plutons, comparison with the experimentally determined phase diagrams of Whitney (1975b) for a synthetic quartz monzonite (adamellite in the IUGS classification) shows that the Basin Creek granitic rocks would have contained less than 4 weight percent water with no vapor phase generated until low temperatures were reached. The components of the high temperature (above 700°C) system are plagioclase, alkali feldspar, quartz, and liquid. The crystallization sequence is plagioclase, alkali feldspar, and then quartz. The addition of biotite to the experimental system suggests that less than 1.5 weight percent water is in the granitic magmas (Wyllie and others, 1976). At 2 kbar, the experimentally determined crystallization sequence is plagioclase, alkali feldspar, quartz, and finally biotite, with no vapor generated until 700°C.

EVOLUTION OF THE PEGMATITES

During crystallization of granitic magma, volatile concentration and vapor pressure increase until the second boiling point is reached (Hyndman, 1972). The water-rich fluid that boils off crystallizes in fractures as pegmatite dikes. Jahns and Burnham (1969) show that at 5 kbar load pressure, a granitic magma with 0.5 weight percent water in solution increases its water content to 11 weight percent when 95 percent of the original magma is crystallized. Crystallization increases the original water content of the melt 22 times. A lowering of atmospheric pressure on the granitic magma to 2 kbar decreases the amount of water dissolved in the magma to 6.5 weight percent (Burnham and Jahns, 1962). Consequently, decreasing load pressure increases the water content of the residual fluid by nearly 50 percent. If the initial granitic magma contains 1.5 weight percent water, as established above, then with cooling and upward emplacement of the granite, an increase in water content within the residual fluid should increase by a factor of

20 to contain 30 weight percent water.

The pegmatites in the Basin Creek area contain few hydrous minerals. The water in the pegmatitic fluids diffused into the host rocks during crystallization of the pegmatites, concentrating the silicate portion of the residual fluid. The water diffused from the pegmatite dikes may have formed the alteration found around many areas of pegmatitic intrusion. Volatiles within the pegmatitic fluids were concentrated by a similar factor of 20. The presence of water within the fluid inhibited nucleation of silicate minerals, forming the coarse-grained pegmatitic texture common to many of the granitic dikes.

DISCUSSION

If the constraints of comparing simple, closed system experiments on granite crystallization are accepted, an upper limit of 1.5 weight percent water content can be established for the Basin Creek rocks. This conclusion agrees with that reached by Maaløe and Wyllie (1975). Progressive crystallization of granitic magma containing 1.5 weight percent water at 2 kbar pressure or 7 km depth will yield a residual fraction of water-saturated silicate liquid with 30 weight percent water (Jahns and Burnham, 1969). Further concentration of the silicate liquid occurs as the water diffuses into the host rocks during crystallization of the pegmatites which are ultimately anhydrous.

CHAPTER V

GEOCHRONOLOGY

Four isotopic dates were obtained on rocks within the Basin Creek area. Two potassium-argon whole-rock dates were from samples of the Cretaceous granitic rocks (hosts of the uranium mineralization), and two uranium-lead dates were on uraninite from the granitic-hosted uranium deposits. Locations of the dated material are shown on Figure 30. The objective of these isotopic dates is to aid in interpretation of the age relationship between uranium-bearing veins and their granite hosts in the Stanley area.

POTASSIUM-ARGON DATES

Porphyritic K-feldspar granite (EBC-48) and quartz granite porphyry (BB-73) are samples from the two granitic units that were isotopically dated by the potassium-argon whole-rock method. In hand sample, BB-73 is a chloritically altered granite from the Lightning Number 2 prospect on Hay Creek. EBC-48 is a fresh-looking sample from a road cut on the Salmon River east of Lower Harden Creek. The sample is lithologically similar to the country rock of most of the granitic-hosted uranium deposits of the area. Table 3 presents the potassium-argon whole-rock data.

These two potassium-argon dates are significantly younger than the two 79 ± 2 m.y. and one 82 ± 2 m.y. potassium-argon biotite dates of Armstrong (1975a) for three nearby samples. There are several reasons for this apparent discordance. Different minerals cool and lock

Figure 30: Isotopic date sample locations.

EXPLANATION

Quaternary

Alluvium

Tertiary

Silicic dike

Rhyolite

Volcanics- undivided

Arkose

Cretaceous

Leucocratic granite

K-feldspar porphyritic granite

Quartz granite porphyry

Equigranular granite

Paleozoic

Xenolith

SYMBOLS

Fault

Contact

Topographic high point

Uranium-lead date

Potassium-argon date

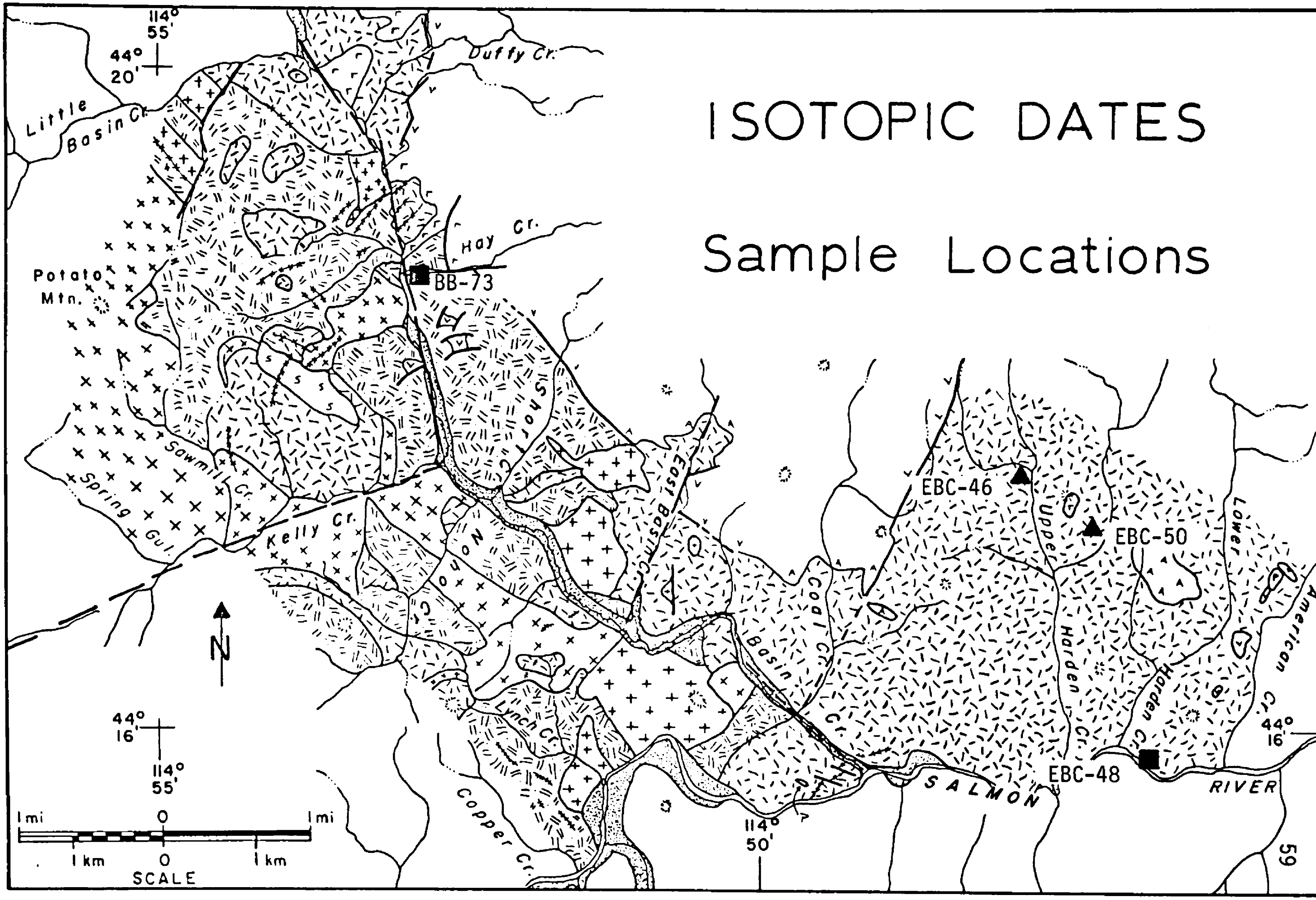

ISOTOPIC DATES
Sample Locations
BB-73
EBC-46
EBC-50
EBC-48
Duffy Cr.
Hay Cr.
Little Basin Cr.
Potato Mtn.
Sawmill Cr.
Spring Gul.
Kelly Cr.
East Basin Cr.
Coal Cr.
Basin Cr.
Upper Harden Cr.
Harden Cr.
Lower American Cr.
Lynch Cr.
Copper Cr.
SALMON RIVER
114° 55'
44° 20'
44° 16'
114° 50'
1 mi 0 1 mi
1 km 0 1 km
SCALE
N

Table 3. Potassium-argon whole-rock dates of samples from the Idaho batholith in the Basin Creek area, Custer County, Idaho.

Sample Number	% K	scc Ar^{40Rad}/ gmz 10^{-5}	% Ar^{40Rad}	Isotopic Age (m.y.)
BB-73	2.72	0.743	86.3	68.7 ± 3.4
	2.73	0.741	89.1	
EBC-48	2.75	0.753	88.5	69.1 ± 3.5
	2.75	0.754	88.4	

Ages calculated using the following constants:

$\lambda_\varepsilon = 0.581 \times 10^{-10} yr^{-1}$

$\lambda_\beta = 4.962 \times 10^{-10} yr^{-1}$

$K^{40} = 1.167 \times 10^{-4}$ atom per atom of natural potassium.

Sample locations:

BB-73 Near center, section 1, T. 11 N., R. 13 E., Lightning Number 2 prospect.

EBC-48 Southeast, section 23, T. 11 N., R 14 E., Roadcut north of the Salmon River and east of Lower Harden Creek.

Analyst: Teledyne Isotopes, Westwood, New Jersey.

radiogenic argon into their systems at different temperatures within a crystallization event. Younger dates may also reflect argon loss because of later alteration or deformation of the dated mineral. Both EBC-48 and BB-73 contain significant amounts of K_2O (see Table 1); most of that potassium is tied up in potassium feldspars. Feldspars are subject to large losses of the radiogenic argon gas (York and Farquhar, 1972). Argon escape is connected with the unmixing of different feldspar phases (perthitization) as the feldspars adjust to lower temperature equilibrium conditions (Sardarov, 1957). In both samples orthoclase contains perthitic streaks visible in thin section. Because argon migrates easily at low temperatures within perthitic feldspar, a rock containing more potassium feldspar than biotite as its major potassium mineral shows lower potassium-argon whole-rock dates relative to a mica date for the same rock (Armstrong, 1966; Damon, 1968). Potassium feldspars regularly show argon loss in undisturbed environments (York and Farquhar, 1972); argon loss from potassium feldspars is greater in disturbed environments. Both BB-73 and EBC-48 show strained quartz and orthoclase in thin section, suggesting these rocks have been deformed.

Whole-rock dating by the potassium-argon method gives an average age which is a composite of the individual mineral dates (York and Farquhar, 1972). If some of the constituent minerals are poor argon retainers, the whole-rock age will be low and will be proportional to the relative abundances of the various minerals and their potassium concentrations. Whole-rock dating of a granite is misleading because of the presence of significant amounts of potassium feldspar which is inevitably subjected to argon loss. Argon loss from the whole-rock samples may have been from later alteration of the rocks (possibly hydrothermal alteration) or reheating after crystallization (possibly related to Eocene igneous activity). There may be one or more factors influencing the assumed argon loss reflected by the low dates reported here. However, these dates presumably place a minimum age on the rock.

URANIUM-LEAD DATES

Two uranium-lead mineral dates were obtained on uraninite within the Basin Creek area. EBC-46 was taken from the face of the open pit at the Hardee prospect. Both black uraninite and yellow secondary uranium minerals are visible at the sample site. EBC-50 was taken from the discovery pit at the Alta claims. The pit lies along a brecciated fault zone containing iron oxides, lead sulfates, and yellow secondary uranium minerals. The uranium-lead data for the two samples is shown in Table 4. EBC-46 shows discordant dates and exhibits a lead loss pattern especially notable because of an excessively old Pb^{207}/Pb^{206} date. Lead loss from uraninite in EBC-46 probably occurred during alteration or leaching at some point within the lifetime of the uranium mineral (Nier, 1939). Dating of EBC-50 produced reasonably concordant dates.

The Idaho batholith's geologic age is Mesozoic and probably Jurassic or Cretaceous (Hyndman, 1979b). On the basis of radiometric ages, Armstrong and others (1977) state that the bulk of the Atlanta lobe of the Idaho batholith is of Late Cretaceous age, 75 to 100 m.y. old, but Eocene magmatic-hydrothermal activity and/or uplift and erosion over broad areas have clouded the isotopic record of Mesozoic events. When

Table 4. Uranium-lead analyses of samples from uranium prospects in the Idaho batholith in the Basin Creek area, Custer County, Idaho.

Sample Number	Uranium (ppm)	Lead (ppm)
EBC-46	4260	81.7
EBC-50	8140	216

	Isotopic Pb (atom %) measured			
	Pb^{204}	Pb^{206}	Pb^{207}	Pb^{208}
EBC-46	0.485	75.166	9.821	14.528
EBC-50	1.291	43.034	14.839	40.836

	Isotopic Pb (troilite corrected)		
	Pb^{206}	Pb^{207}	Pb^{208}
EBC-46	93.308	6.378	0.314
EBC-50	87.746	4.384	7.870

	Pb^{206}/U^{238} (m.y.)	Pb^{207}/U^{235} (m.y.)	Pb^{207}/Pb^{206} (m.y.)	Pb^{207}/Pb^{206}
EBC-46	133	182	901	0.0684
EBC-50	172	174	195	0.0499

Sample locations:

EBC-46 Southeast, section 10, T. 11 N., R. 14 E., Hardee prospect.

EBC-50 Northwest, section 14, T. 11 N., R. 14 E., Alta prospect.

Analyst: Teledyne Isotopes, Westwood, New Jersey.

compared with the generally accepted age for the Atlanta lobe, both uranium-lead uraninite mineral dates appear significantly older than their granitic host rocks. This may be the result of pre-existing lead being incorporated into the uraninite structure during crystallization of the mineral (Koeppel, 1968). However, uranium deposits generally do not contain common or non-radiogenic lead (Doe, 1970). Uraninite in fractures and cracks is easily affected by tectonic activity and may give anomalous or misleading dates. The apparent old age of uranium mineralization within the Basin Creek area (compared to potassium-argon mineral dates on the granitic hosts) is probably due to the presence of "older" lead within uraninite that had to have been deposited after its host rock was formed. Lead ratios often do not change at the time of mineralization (Kanasewich, 1968) so that these dates may well reflect lead ages of the uranium source, or an intermediate age between the initial age of the lead and a resetting event.

CHAPTER VI

URANIUM MINERALIZATION

In the Stanley area, uranium concentrations occur within the Idaho batholith and within the overlying arkosic sediments at the base of the Tertiary section. The granitic and arkosic occurrences may be genetically related, but no one has studied this relationship. The arkosic occurrences have a greater economic potential, but I am concerned here only with the granitic occurrences.

GENERAL STATEMENT

Three types of mineralization are found within the batholithic rocks: veins, pegmatites, and stockwork. All uranium mineralization is structurally controlled. Veins host chalcedony or fine-grained quartz with stringers of uraninite. They are variable in size, density, and extent. Pegmatites are particularly anomalous at intersections with faults. Stockwork uraninite occurs along tiny fractures within the granitic rock which locally appear to be closely spaced.

Uranium mineralogy is complex and accurate only with x-ray identification. Common uranium minerals may be divided into three general groups: black, yellow, and green. Uraninite $((U^{+4},U^{+6})O_2)$ is the most common black mineral; yellow minerals may be any of a host of secondary uranium minerals, but, within the Stanley area, appear to be uranophane (calcium and hexavalent uranium hydrated silicate, an alteration of uraninite). Autunite (calcium and hexavalent uranium hydrated phosphate) is the most widespread green mineral. Pitchblende is a slightly more

Figure 31: Uranium occurrences in the Idaho batholith, Basin Creek area.

EXPLANATION

Quaternary

Alluvium

Tertiary

Silicic dike

Rhyolite

Volcanics- undivided

Arkose

Cretaceous

Leucocratic granite

K-feldspar porphyritic granite

Quartz granite porphyry

Equigranular granite

Paleozoic

Xenolith

SYMBOLS

Fault

Contact

Topographic high point

Uranium occurrence

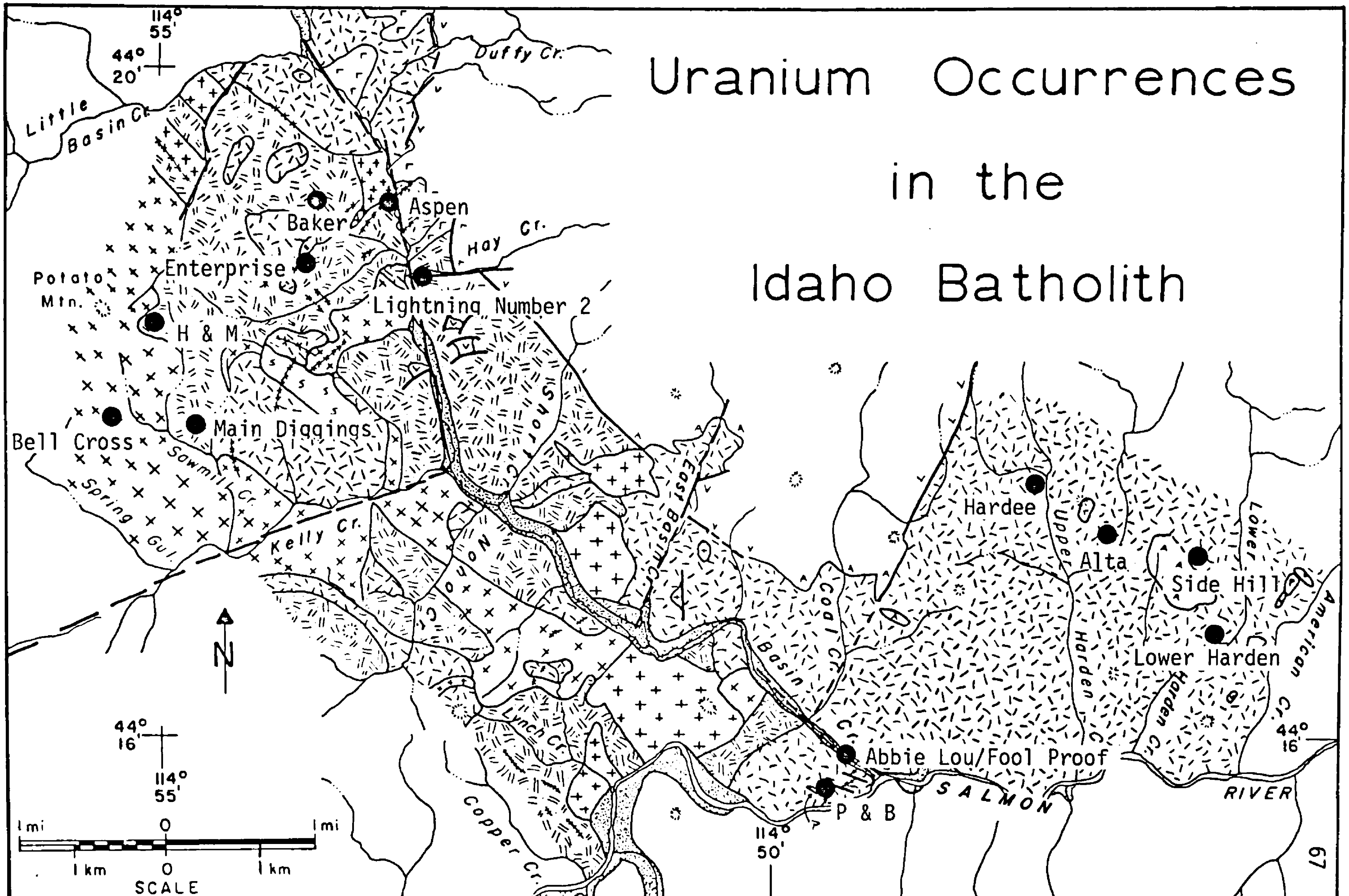
Uranium Occurrences in the Idaho Batholith
Aspen
Baker
Enterprise
Lightning Number 2
H & M
Main Diggings
Bell Cross
Hardee
Alta
Side Hill
Lower Harden
Abbie Lou/Fool Proof
P & B
Potato Mtn.
Little Basin Cr.
Duffy Cr.
Hay Cr.
Sawmill Cr.
Spring Gul.
Kelly Cr.
Moyer Cr.
Snyder Cr.
East Basin Cr.
Coal Cr.
Basin Cr.
Lynch Cr.
Copper Cr.
Upper Harden Cr.
Harden Cr.
Lower American Cr.
SALMON RIVER
N
114° 55'
44° 20'
44° 16'
114° 50'
1 mi 0 1 mi
1 km 0 1 km
SCALE

oxidized variety of uraninite containing less than 0.1% thorium and rare-earth elements (Elevatorski, 1978). The only distinguishing feature between pitchblende and uraninite in hand specimen is a subtle difference in luster. Pitchblende has a pitch-like luster and uraninite has a sub-metallic to iron-like luster. I have field identified the visible primary black uranium mineral in the Basin Creek area as uraninite because of its sub-metallic luster. I did not further investigate the mineralogy of the uranium.

STANLEY AREA PROSPECTS

Numerous uranium claims have been located within the Stanley area since the early 1950's. Some of these are on potentially significant uranium occurrences, and others cover minor anomalies. Kern (1959) and Choate (1962) provide detailed descriptions of all uranium claims in the Stanley area. The three types of uranium mineralization found within the Idaho batholith are discussed with examples drawn from the thesis area. All types may be found together or separately - age relationships are unknown.

Veins

The best examples of uranium-bearing veins are found at the Alta and Hardee prospects (Plate I and Figure 31) within the Upper Harden Creek drainage. Fine-grained uraninite occurs disseminated in chalcedony stringers (Figure 22, page 33) within fractures and faults. The veins and veinlets of chalcedony and uraninite are everywhere found within pre-existing structures that are subparallel to the regional structural grain. Surface manifestations of uranium-bearing vein occurrences are typically altered and oxidized with iron and manganese oxides, clays, and secondary uranium minerals. Primary, unoxidized mineralization increases with depth from the surface, as is observed traversing the Alta and Hardee adits.

Pegmatites

Strongly anomalous radioactivity is characteristically associated where pegmatites intersect faults near uranium-bearing veins. Mineralization was not observed in any pegmatites; gamma-ray spectrometer anomalies may be controlled by the dominance of potassium or thorium radiation and not necessarily uranium radiation. The highest radioactivity readings at the Alta prospect (twenty to forty times background) were found at the intersection of a fault and several thick (0.5 to 2 meters) pegmatites. Anomalous pegmatites also occur at the Abbie Lou/Fool Proof, Baker, Bell Cross, and Hardee prospects.

Stockwork

Stockwork uranium occurs within the granitic rocks as fine-grained uraninite along microfractures. The Hardee adit exposes the best examples of this type of mineralization. Concentrations of the microfractures appear to be moderate with twenty to forty fractures per meter. Economic mineralization may be encountered where microfractures occur in a dense stockwork.

Structural Control

Structural control is crucial to uranium mineralization in the granitic rocks. The major mineralized structures trend N30°W, N45°W, N75°W, and N65°E and dip at high angles (Figure 32). The structures may be en echelon and discontinuous along a trend, or narrow or continuous, as at the Hardee prospect. Uraninite has been localized within the fractured and therefore more permeable rock. Uranium minerals are commonly not found within large faults (0.5 to 1 meter wide) but within fractures and joints near the faults. The faults probably were the hydrothermal conduits for the mineralizing fluids, but later movement and/or passage of fluids may have removed any evidence of mineralization. However, fault gouge may have been too impermeable to permit hydrothermal solutions to move along the fault zones, forcing the solutions to move along nearby fractures and joints.

Host Rock Preparation for Mineralizing Solutions

As observed in the granitic rock descriptions (Chapter III), much of the Basin Creek area has been altered, both deuteric/hydrothermal and surficial alteration. Surficial weathering is continuing, but the timing for deuteric/hydrothermal alteration is ambiguous. Deuteric alteration may have occurred as late-stage magmatic fluids circulated through the hot pluton(s), and/or hydrothermal alteration may have occurred later (in Eocene time?), in conjunction with circulating uraniferous fluids. Fine-grained white micas, chlorite, and epidote indicate a low-temperature alteration suite. The areas around the Basin Creek uranium occurrences are generally more altered than areas far away, such as near the confluence of Little Basin Creek and Basin Creek at the north end of the thesis area. The altered granite has a strong greenish hue compared with an otherwise gray rock.

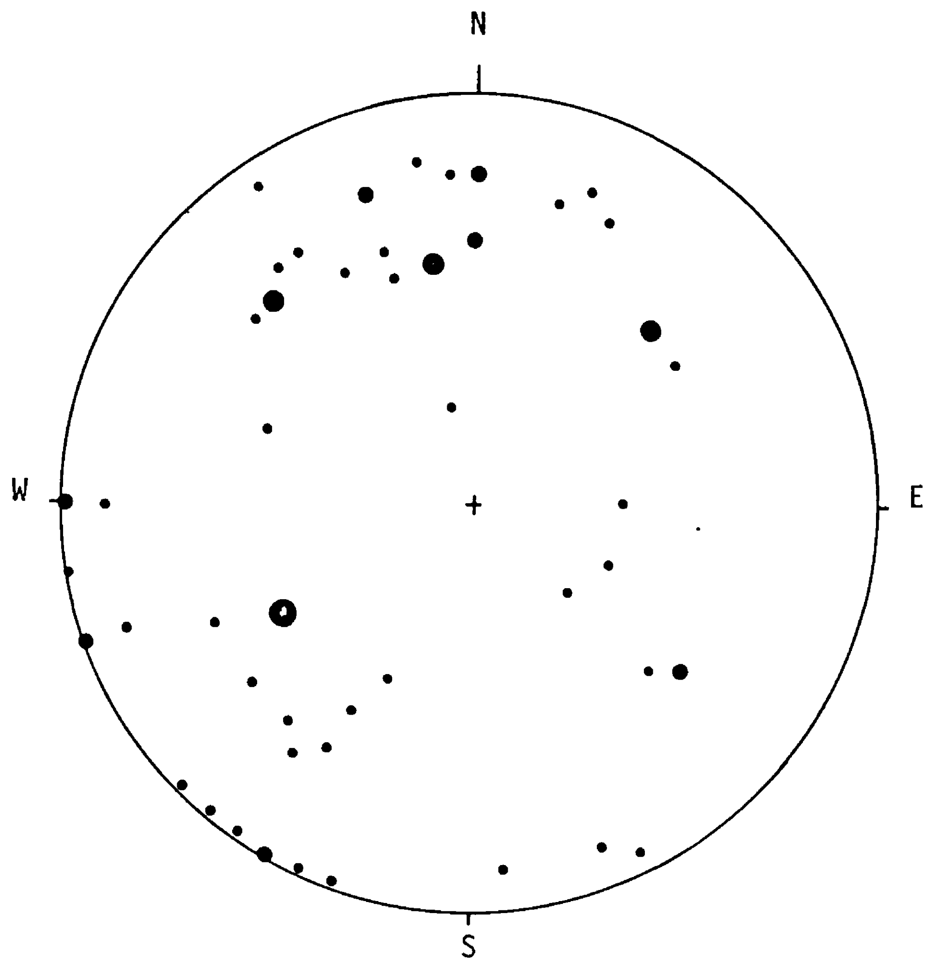

Figure 32: Stereographic projection of poles to mineralized structures at the Alta, Bell Cross, Baker, Hardee and Lightning Number 2 prospects.

A greater density of fractures is observed in areas of uranium mineralization than elsewhere. These fractures often display evidence of some movement. The fractures have red discoloration, iron-stain coatings and pyrolusite dendrites along their surfaces.

One set of uranium-bearing fractures in the Fool Proof prospect is located fifty meters northwest of an active hot spring. The spring is localized along a Tertiary rhyolite dike which has been offset by a fault controlling the lower part of the Basin Creek drainage. No hydrothermal alteration is visible adjacent to the spring because of vegetative cover. The chalcedony-uraninite veinlets may be related to the hot spring system. Hot springs are found throughout the Stanley area. Hot springs are surface manifestations of an area of high heat flow, probably since the Eocene and perhaps since the Cretaceous. Other uraninite veins in the Basin Creek area may have an origin related to an anomalous heat system.

URANIUM DEPOSITS IN GRANITIC ROCKS

Granites contain four times (3 to 4 ppm) as much uranium as do basic igneous rocks; certain granites such as the peralkaline albite-riebeckite granite of the Kaffo Valley in Nigeria and the alkali-rich Conway granite of New Hampshire contain 10 to 12 ppm uranium (Bowie, 1970). Along with high uranium backgrounds, uranium may be further concentrated in various deposits within granitic rocks. These include uraniferous veins, pegmatites, alaskites, and "high-grade" granites. Examples of each type of deposit are discussed below.

At Bancroft, Ontario, Canada, uraninite-thorite veins and irregular lenses cut and replace bodies of unzoned granitic pegmatites within highly metamorphosed Precambrian sedimentary rocks (Finch and others, 1973). These are the only granitic pegmatites in the world that have been extensively worked for uranium.

The Rossing deposit, South West Africa, is the world's largest known uranium deposit in pegmatitic alaskites. Primary and secondary uranium minerals are disseminated within a migmatitic granite (von Backstrom, 1970). The uranium is thought to be genetically related to the Cambro-Ordovician anatectic granites (Rogers, 1977).

At the Ross-Adams Mine, in southeast Alaska, a low-grade, large-tonnage, "porphyry" uranium deposit is hosted by peralkaline riebeckite granite. There are no sharp contacts between ore and host granite. Ore occurs as disseminations and segregations of uranium minerals in the granite; the uranium minerals appear to have become more concentrated in later phases of crystallization (MacKevett, 1963).

Other areas of plutonic-hosted uranium deposits include the bostonite dikes of the Colorado Front Range; anatectic(?) pegmatites and aplites of Radium Hill, Australia; uranium-bearing hydrothermal vein deposits in the Boulder batholith, Montana; pegmatites and alaskites of Mount Spokane, Washington; and Midnite Mine, Washington, where uranium is concentrated in a metasedimentary roof pendant within a granitic stock (Mickle and Mathews, 1978). F. C. Armstrong (1974) describes hypothetical "porphyry" uranium deposits as orebodies of 400 ppm uranium disseminated within and along fractures and shears in granitic rock. Suitable host rocks are alaskite, leucocratic granite, and biotite granite that contain a complex network of aplitic and pegmatitic dikes of quartz and

K-feldspar. Uranium generally occurs as primary uraninite and/or ionic and molecular disseminations of uranium.

CHAPTER VII

DISCUSSION

The Basin Creek area is similar to the Boulder batholith of western Montana (Castor and Robins, 1978). Uranium mineralization occurs in both areas within composite granitic intrusions of Late Cretaceous age. Both the Idaho and Boulder batholiths locally host uranium occurrences of several types. The Basin Creek region of the Idaho batholith hosts pegmatitic occurrences, uraninite-chalcedony veins, and stockwork ("porphyry") occurrences. The Boulder batholith hosts these three types of mineralization as well as uranium in base metal sulfide veins (Bieler and Wright, 1960).

Pegmatitic occurrences are highly differentiated, residual magmas enriched in uranium and volatiles which have been expulsed from cooling differentiated melts (Adler, 1977) and injected into older host rocks. At Basin Creek the pegmatitic host rocks are the earlier pulses of the Idaho batholith: equigranular granite, K-feldspar porphyritic granite, and quartz granite porphyry. No pegmatites have been observed in the late-stage leucocratic granite and the relationship between pegmatites and leucocratic granite is unknown. Discussion in Chapter IV has demonstrated a 20-times increase in the water content within residual fluids derived from a water-undersaturated granitic magma. A similar increase in volatile content would yield a concentration of uranium from an average of 6.3 ppm (Table 5) to 126 ppm.

Uraninite-chalcedony veins are younger than their host rocks;

Table 5. Background uranium values for selected specimens of Basin Creek rocks.

U ppm	Sample Number	Rock Description
9.6	EBC-47	Altered K-feldspar porphyritic granite.
4.5	EBC-48	Fresh K-feldspar porphyritic granite.
6.9	EBC-49	Fresh hornblende-bearing K-feldspar porphyritic granite.
3.0	BB-70	Fresh quartz granite porphyry.
5.6	BB-73	Altered quartz granite porphyry.
7.0	EBC-52	Altered leucocratic granite.
3.0	EBC-53	Fresh leucocratic granite.

Analyst: Noranda Exploration Co. Ltd., Vancouver, British Columbia, Canada.

structural control is important in trapping the uranium-bearing hydrothermal solutions. The veins commonly display textures of open-space filling within faults, joints or fracture zones (Rich, Holland, and Petersen, 1977). The uraninite-chalcedony veins at Basin Creek are structurally controlled along northwesterly trends. This dominant trend occurs within the batholithic rocks but is not observed in the nearby Challis volcanics, suggesting that the northwest grain is pre-Challis and therefore pre-Eocene and was not active during Challis events. Choate's (1962) descriptions of the veins suggest open-space filling textures for the vein material. Rich, Holland, and Petersen (1977) observe that most hydrothermal uranium deposits in the United States are hosted by competent felsic igneous and metamorphic rocks of Precambrian, Late Mesozoic, and Tertiary age. The authors also note a strong positive correlation between the distribution of uraninite veins and granites containing anomalously large amounts of uranium of greater than 5 ppm. The uraninite-chalcedony veins of the Boulder batholith contain 95% quartz (Wright and Bieler, 1960); many of the radioactive veins at the Alta prospect at Basin Creek are composed predominantly of chalcedony with microscopic blebs of uraninite (Kern, 1959).

Uranium is generally enriched in the youngest and most felsic members of the granitic suite (Bohse and others, 1974; Rogers and others, 1978). If the uranium-bearing volatile phase separates from the magma, pegmatite or hydrothermal vein deposits may form elsewhere in suitable traps. If the volatile phase is retained during crystallization of a water-saturated, highly differentiated magma, a high concentration of uranium is disseminated within the plutonic rock or concentrated in a stockwork of fractures. This may form a uranium occurrence of low-grade, large-tonnage potential. The uranium may occur as primary uranium-bearing minerals, in micro-inclusions, and in intergranular "films" (Sorensen, 1977, p. 49). The Ross-Adams alkali granite in southeastern Alaska is a classic example of a granite that contains abnormal amounts of late-stage volatiles: uranium, thorium, yttrium, lanthanum, nickel, cesium, and rare-earth elements (von Backstrom, 1974). Dissemination of uranium along microfractures in the Hardee prospect at Basin Creek may be comparable to the hypothetical "porphyry"-type occurrences of F. C. Armstrong (1974). At the Hardee, uraninite may have been remobilized and concentrated along tiny fractures proximal to the larger uraniferous veins. However, the host K-feldspar porphyritic granite is not the youngest nor most differentiated phase exposed in the Basin Creek sequence. Therefore, if the uranium is genetically related to a late-stage differentiate of the batholith, its source rock is elsewhere within the Idaho batholith.

The leucocratic granite of the Basin Creek area is probably not the uranium source rock because it presently has a uranium content one-and-one-half to three times less than the background values for the quartz granite porphyry or K-feldspar porphyritic granite units (see Table 5). Rich and others (1977) observe that highly radioactive granites (>10 ppm) often have closely associated hyrothermal uranium deposits. This suggests that anomalous granites are the uranium sources for the hydrothermal deposits. Quartz granite porphyry and K-feldspar porphyritic granite are the most likely granitic sources for the granitic-hosted uranium deposits in the Basin Creek area.

TERTIARY URANIUM SOURCES

The uranium-lead isotopic dates for uraninite from the Basin Creek area (discussed in Chapter V) indicate that the uranium was probably remobilized within the Cretaceous granite from Idaho batholith source rocks and/or country rocks, but the age of the granitic-hosted uraninite veins is not known. There are few geologic constraints to limit speculations on the age and genesis of the uraninite vein deposits. Both the Idaho batholith and overlying Tertiary arkose are uraniferous host rocks, but I do not know if both rock types were mineralized during the same event. I have discussed, above, a plausible Cretaceous mineralizing event. Several workers have suggested that much of the mineralization found in Idaho is related to Tertiary plutonism (Anderson, 1951; Bennett, 1980); if this is the case for the Stanley uranium deposits, they may be related to the local Tertiary plutons: Sawtooth batholith, 15 km to the south-southwest, and Knapp Peak pluton, 20 km to the north-northwest. Tertiary plutons within the Idaho batholith contain twice as much K^{40}, U, and Th as the main batholith (Swanberg and Blackwell, 1973). Much of the uranium occurs in hydrous and secondary minerals resulting from interaction with meteoric ground waters (Gosnold, 1977). The Tertiary epizonal plutons set up large convective hot-water systems (Criss and Taylor, 1978) that could have circulated uraniferous fluids through the Tertiary plutons, Cretaceous granite, and arkosic sediments. If all the uranium occurrences in the Basin Creek area are the same age, a Tertiary source and genesis is probable.

The oxygen and hydrogen isotope studies of Taylor (1978) show that most of the Atlanta lobe of the Idaho batholith has been affected by meteoric/hydrothermal activity. Fehn and others (1978) discuss three mechanisms to hydrothermally redistribute metals within granitic plutons. Each mechanism is capable of developing a hydrothermal uranium deposit. The hydrothermal convection mechanisms are: 1) initial heat of the pluton (Cretaceous event); 2) later addition of heat from nearby thermal disturbances (Tertiary epizonal plutons); and 3) thermal anomalies related to radioactive decay. Radioactive decay within central Idaho occurs in both the Cretaceous and Tertiary granitic plutons but especially in the latter as noted above. The mass of water convected by radioactive heat generation during a few million years is comparable to the mass of water convected by a cooling intrusive (Fehn and others, 1978). If hydrothermal convection from radioactive heat generation has created the uranium deposits in the Basin Creek area, why do only the Idaho batholith and Tertiary arkose contain economic concentrations of uranium? The Challis volcanics apparently do not host any economic uranium occurrences (Siems and others, 1979). This question goes beyond the scope of this thesis, but it seems that the Idaho batholith and Tertiary arkose provided optimal settings for uranium deposition and concentration.

The granitic-hosted uranium occurrences in the Basin Creek area are located close to the contact with the Tertiary arkose. The arkose developed on an erosional surface of the Idaho batholith in early

Tertiary time. The vein occurrences display textures of open-space filling, strong structural control, and a low-temperature hydrothermal mineralogy (Kern, 1959), including stibnite. All uranium occurrences in the Basin Creek area may have formed under near-surface conditions (less than 3 km; Cater and others, 1973, p. 23) beneath the Challis volcanic pile. Convection cells set up around the recently intruded Tertiary Sawtooth and Knapp Peak plutons circulated uraniferous groundwaters through permeable zones. In the Basin Creek area the most permeable zone was the unconformity between the arkosic sediments and the fractured Idaho batholith. Because quartz granite porphyry and K-feldspar porphyritic granite host the majority of uranium vein occurrences, these two units must have formed the surface of unconformity. The uraniferous meteoric waters descended along fractures, joints, and faults intersecting the surface of unconformity to form supergene deposits. The source of the uranium was the Challis igneous rocks (both intrusive and extrusive). This supergene mechanism of mineralizing the Idaho batholith contrasts the Tertiary hypogene mechanism suggested by several authors for the Basin Creek area: Kern (1959) and Choate (1962).

CHAPTER VIII

SUMMARY AND CONCLUSIONS

The Basin Creek area is located on the eastern fringe of the Atlanta lobe of the Idaho batholith where a variety of textural phases are exposed. Several magmatic pulses along the eastern edge of the batholith fit into a chronologic framework that displays an apparent evolution of magma from intermediate to felsic compositions. The five textural and compositional units of the Idaho batholith are:

Equigranular Granite
Quartz Granite Porphyry
K-feldspar Porphyritic Granite
Leucocratic Granite
Aplites and Pegmatites.

Leucocratic granite is a late-stage differentiated phase of Cretaceous intrusive activity which is not anomalous in uranium content or mineralization, as might be anticipated for a differentiated magma. K-feldspar porphyritic granite contains the best granitic-hosted uranium deposits in the Stanley area. Quartz granite porphyry and pegmatite dikes are also good uranium host rocks.

The genetic relationship between the Idaho batholith and its uranium mineralization is uncertain; the uranium mineralization is later than and structurally controlled within the granitic rocks. Origin of the uranium is ambiguous, particularly when considering the much greater age of the uranium-lead isotopic data. Several mechanisms for generating uranium deposits within the granitic rocks are presented in Chapters VI and VII. Uranium may be concentrated in the residual melt which becomes water-saturated with continued crystallization of a water-undersaturated granitic magma. Emplacement of the uranium in water-saturated, volatile-rich liquid may form the three types of granitic-hosted uranium deposits found in the Basin Creek area: hydrothermal veins, pegmatites, and stockwork.

Tertiary epizonal plutons within the Idaho batholith appear to have created large convective hot water systems which circulated uraniferous fluids. The uranium could have been leached from high uranium background rocks: Cretaceous K-feldspar porphyritic granite, Cretaceous quartz granite porphyry, Tertiary granite, or Tertiary felsic volcanics. Emplacement of the uranium as hypogene or supergene deposits may have occurred as a single event or as several events, related to Cretaceous and/or Eocene igneous activity. Although the genetic relationship between the Idaho batholith and its uranium mineralization can not be proven, the relationship has been shown to be plausible given the conditions observed in the Basin Creek area of the Idaho batholith.

SPECULATIONS

In conclusion, I submit several speculations on the Basin Creek geology. The Stanley area is the only significant area of known uranium mineralization in the Idaho batholith because of special favorable conditions which include: proper ground preparation, source of uranium and hydrothermal fluids, conduits and mechanisms to circulate fluids, and reducing chemical conditions favorable for uranium precipitation. Other areas of the Idaho batholith may be mineralized but erosion has removed or not yet exposed those mineralized areas.

The leucocratic granite is similar in appearance to the White Cloud and Thompson Creek stocks. Both Late Cretaceous stocks host significant stockwork-molybdenum minerals. Because of the similarity, the leucocratic granite makes a good molybdenum exploration target. However, the leucocratic granite does not display an appropriate alteration suite of sericite, pyrite, silicification, and/or potassic alteration.

The Tertiary rhyolite and silicic dikes are part of the Idaho porphyry belt and/or are surface manifestations of buried Tertiary plutons. Kiilsgaard (verbal communication, 1978, in Bennett, 1980) has traced Tertiary dikes into a Tertiary pluton along the South Fork of the Payette River near Lowman. A similar situation may exist for the Basin Creek dikes providing a local Tertiary heat system to circulate uraniferous fluids in the Idaho batholith and the Tertiary arkosic sediments.

REFERENCES CITED

Adler, H. H., 1977, Geochemical factors contributing to uranium concengration in alkalic igneous rocks, in Recognition and evaluation of uraniferous areas: Vienna, Int'l. Atomic Energy Agency, p. 35-43.

Anderson, A. L., 1951, Metallogenic epochs in Idaho: Econ. Geol., v. 46, p. 592-607.

Armstrong, F. C., 1974, Uranium resources of the future - "porphyry" uranium deposits, in Formation of uranium ore deposits: Vienna, Int'l. Atomic Energy Agency, p. 625-634.

Armstrong, R. L., 1966, K-Ar dating of plutonic and volcanic rocks in orogenic belts, in Schaefer, O. A., and Zahringer, J., Potassium argon dating: New York, Springer-Verlag, p. 117-133.

_____ 1974, Geochronometry of the Eocene volcanic-plutonic episode in Idaho: Northwest Geology, v. 3, p. 1-15.

_____ 1975a, The geochronometry of Idaho: Isochron/West, no. 14, 50 p.

_____ 1975b, Precambrian (1500 m.y. old) rocks of central Idaho - the Salmon River Arch and its role in Cordilleran sedimentation and tectonics: Amer. Jour. Sci., v. 275-A, p. 437-467.

Armstrong, R. L., Taubeneck, W. H., and Hales, P. O., 1977, Rb-Sr and K-Ar geochronometry of Mesozoic granitic rocks and their Sr isotopic composition, Oregon, Washington, and Idaho: Geol. Soc. Am. Bull., v. 88, p. 397-411.

Barker, D. S., 1970, Compositions of granophyre, myrmekite, and graphic granite: Geol. Soc. Am. Bull., v. 81, p. 3339-3350.

Bennett, E. H., 1973, The petrology and trace element distribution of part of the Idaho batholith compared to the White Cloud stock, Custer County, Idaho: Ph.D. dissert., Univ. Idaho, Moscow, 172 p.

_____ 1980, Granitic rocks of Tertiary age in the Idaho batholith and their relation to mineralization: Econ. Geol., v. 75, p. 278-288.

Bieler, B. H., and Wright, H. D., 1960, Primary mineralization of uranium-bearing "siliceous reef" veins in the Boulder batholith, Montana: Part II - the veins: Econ. Geol., v. 55, p. 363-382.

Bohse, H., Rose-Hansen, J., Sorensen, H., Steenfelt, A., Lorborg, L., and Kunzendorf, H., 1974, On the behavior of uranium during crystallization of magmas - with special emphasis on alkaline magmas, in Formation of uranium ore deposits: Vienna, Int'l. Atomic Energy Agency, p. 49-60.

Bond, J. G. (compiler), 1978, Geologic map of Idaho: Idaho Bur. Mines & Geol., scale 1:500,000.

Bowie, S. H. U., 1970, Some geological concepts for consideration in the search for uranium provinces and major uranium deposits, in Uranium exploration geology: Vienna, Int'l. Atomic Energy Agency, p. 285-297.

Burnham, C. W., and Jahns, R. H., 1962, A method for determining the solubility of water in silicate melts: Amer. Jour. Sci., v. 260, p. 721-745.

Carmichael, I. S. E., Turner, F. J., and Verhoogen, J., 1974, Igneous petrology: New York, McGraw-Hill, 739 p.

Castor, S. B., and Robins, J. W., 1978, Preliminary study of uranium favorability of the Boulder batholith, Montana: U.S. Dept. of Energy Report, GJBX-5(78), 28 p.

Cater, F. W., and others, 1973, Mineral resources of the Idaho Primitive Area and vicinity, Idaho: U.S. Geol. Survey Bull. 1304, 431 p.

Cavanaugh, P. C., 1979, The geology of the Little Boulder Creek molybdenum deposit, Custer County, Idaho: M.S. thesis, Univ. of Montana, Missoula, 100 p.

Choate, R., 1962, Geology and ore deposits of the Stanley area: Idaho Bur. Mines & Geol., Pamphlet 126, 122 p.

Christiansen, R. L., and Lipman, P. W., 1972, Part 2, Late Cenozoic volcanism and plate tectonic evolution of the western United States: Phil. Trans. R. Soc. London, A, v. 271, p. 249-284.

Cox, K. G., Bell, J. D., and Pankhurst, R. J., 1979, The interpretation of igneous rocks: London, George Allen and Co., 450 p.

Criss, R. E., and Taylor, H. P., Jr., 1978, Regional $^{18}O/^{16}O$ and D/H variations in granitic rocks of the southern half of the Idaho batholith and the dimensions of the giant hydrothermal systems associated with emplacement of the Eocene Sawtooth and Rocky Bar plutons: Geol. Soc. Amer., Abstracts with Programs, v. 10, no. 7, p. 384.

Cross, W., Iddings, J. P., Pirsson, L. V., and Washington, H. S., 1902, A quantitative chemicomineralogical classification and nomenclature of igneous rocks: Jour. Geol., v. 10, p. 555-690.

Damon, P. E., 1968, Potassium-argon dating of igneous and metamorphic rocks with applications to the Basin ranges of Arizona and Sonora, in Hamilton, E. I., and Farquhar, R. M., (eds.), Radiometric dating for geologists: London, Interscience Pub., p. 1-71.

Doe, B. R., 1970, Lead isotopes: New York, Springer-Verlag, 137 p.

Dover, J. H., 1969, Bedrock geology of the Pioneer Mountains, Blaine and Custer Counties, Idaho: Idaho Bur. Mines & Geol., Pamphlet 142, 66 p.

Elevatorski, E. A., 1978, Uranium ores and minerals: Dana Point, California, Minobras, 89 p.

Fehn, U., Cathles, L. M., and Holland, H. D., 1978, Hydrothermal convection and uranium deposits in abnormally radioactive plutons: Econ. Geol., v. 73, p. 1556-1566.

Finch, W. I., Butler, A. P., Jr., Armstrong, F. C., and Weissenborn, A. E., 1973, Uranium, in United States mineral resources: U.S. Geol. Survey Prof. Paper 820, p. 456-468.

Gosnold, W. D., Jr., 1977, A model for uranium and thorium assimilation by intrusive magmas and crystallizing plutons through interaction with crustal fluids: Dissert. Abs. Int'l., v. 38, no. 3, p. B1107.

Hamilton, W., 1976, Tectonic history of west-central Idaho: Geol. Soc. Amer., Abstracts with Programs, v. 8, p. 378-379.

Heinrich, E. W., 1965, Microscopic identification of minerals: New York, McGraw-Hill, 414 p.

Hutchinson, C. S., 1974, Laboratory handbook of petrographic technique: New York, J. Wiley and Sons, p. 414-418.

Hyndman, D. W., 1972, Petrology of igneous and metamorphic rocks: New York, McGraw-Hill, 533 p.

_____ 1979a, Major tectonic elements and tectonic problems along the line of section from northeastern Oregon to west-central Montana: Geol. Soc. Amer. Map Chart Series, MC-28C.

_____ 1979b, The Idaho batholith and associated plutons, Idaho and western Montana, in Roddick, J. R., and Bateman, P. C., eds., Circum-Pacific batholiths (in press).

Hyndman, D. W., Petrology of igneous and metamorphic rocks, 2nd ed., manuscript.

Hyndman, D. W., Badley, R., and Rebal, D., 1977, Northeast-trending early dike swarm in central Idaho and western Montana: Geol. Soc. Amer., Abstracts with Programs, v. 9, no. 6, p. 734.

Jahns, R. H., and Burnham, C. W., 1969, Experimental studies of pegmatite genesis: I. A model for the derivation and crystallization of granitic pegmatites: Econ. Geol., v. 64, p. 843-864.

Johannsen, A., 1939, A descriptive petrography of the igneous rocks, vol. 1: Chicago, Univ. of Chicago Press, 318 p.

Kanasewich, E. R., 1968, The interpretation of lead isotopes and their geological significance, in Hamilton, E. I., and Farquhar, R. M.,(eds.), Radiometric dating for geologists: London, Interscience Pub., p. 147-223.

Kern, B. F., 1959, Geology of the uranium deposits near Stanley, Custer County, Idaho: Idaho Bur. Mines & Geol., Pamphlet 117, 40 p.

Koeppel, V., 1968, Age and history of the uranium mineralization of the Beaverlodge area, Saskatchewan: Can. Geol. Survey Paper 67-31, 111 p.

Larsen, E. S., Jr., 1938, Some new variation diagrams for groups of igneous rocks. Jour. Geol., v. 46, p. 505-520.

Maaløe, S., and Wyllie, P. J., 1975, Water content of a granite magma deduced from the sequence of crystallization determined experimentally with water-undersaturated conditions: Contrib. Mineral. Petrol., v. 52, p. 175-191.

MacKevett, E. A., 1963, Geology and ore deposits of the Bokan Mountain uranium-thorium area, southeastern Alaska: U.S. Geol. Survey Bull. 1154, 125 p.

Marvin, R. F., Tschanz, C. M., Mehnert, H. H., and Mangum, J., 1973, Late Cretaceous age for molybdenite mineralization in Custer County, Idaho: Isochron/West, no. 7, p. 1.

Mickle, D. G., and Mathews, G. W., 1978, Geologic characteristics of environments favorable for uranium deposits: U.S. Dept. of Energy Report, GJBX-67(78), 250 p.

Nier, A. D., 1939, The isotopic constitution of radiogenic leads and the measurement of geologic time, II: Physical Review, v. 55, p. 153-163.

Olson, H. J., 1968, The geology and tectonics of the Idaho porphyry belt from the Boise Basin to the Casto quadrangle: Ph.D. dissert., Univ. Arizona, Tucson, 154 p.

Reid, R. R., 1963, Reconnaissance geology of the Sawtooth Range, Idaho Bur. Mines & Geol., Pamphlet 129, 36 p.

Rember, W. C., and Bennett, E. H. (compilers), 1979, Geologic map of the Challis quadrangle, Idaho: Idaho Bur. Mines & Geol. Geologic map series.

Rich, R. A., Holland H. D., and Petersen, U., 1977, Hydrothermal uranium deposits: Amsterdam, Elsevier, 264 p.

Rogers, J. J. W., 1977, Preliminary report on visit to South West Africa: Appendix 3, 9 p., in Nishimori, R. K., Ragland, P. C., Rogers, J. W., and Greenberg, J. K., Uranium deposits in granitic rocks: Energy Research and Development Administration Report, GJBX-13(77), 93 p.

Rogers, J. J. W., Ragland, P. C., Nishimori, R. K., Greenberg, J. K., and Hauck, S. A., 1978, Varieties of granitic uranium deposits and favorable exploration areas in the eastern United States: Econ. Geol., v. 73, p. 1539-1555.

Ross, C. P., 1934, Geology and ore deposits of the Casto quadrangle, Idaho: U.S. Geol. Survey Bull. 854, 135 p.

_____ 1937, Geology and ore deposits of the Bayhorse region, Custer County, Idaho: U.S. Geol. Survey Bull. 877, 161 p.

_____ 1961, A redefinition and restriction of the term Challis volcanics: U.S. Geol. Survey Prof. Paper 424-C, p. 177-180.

_____ 1963, Modal composition of the Idaho batholith: U.S. Geol. Survey Prof. Paper 475-C, p. 86-90.

Sardarov, 1957, Geochemistry, v. 3, p. 193.

Siems, P. L., Albers, D. F., Malloy, R. W., Mitchell, V. E., and Perley, P. C., 1979, Uranium potential and geology of the Challis volcanics of the Basin Creek-Yankee Fork area, Custer County, Idaho: U.S. Dept. of Energy Report, GJBX-33(79), 137 p.

Sorenson, H., 1977, Features of the distribution of uranium in igneous rocks - uranium deposits associated with igneous rocks, in Recognition and evaluation of uraniferous areas: Vienna, Int'l. Atomic Energy Agency, p. 47-52.

Stern, C. R., Huang, W. L., and Wyllie, P. J., 1975, Basalt-andesite-rhyolite-H_2O: crystallization intervals with excess H_2O and H_2O-undersaturated liquidus surfaces to 35 kilobars, with implications for magma genesis: Earth Planet. Sci. Letters, v. 28, p. 189-196.

Streckeisen, A., 1976, To each plutonic rock its proper name: Earth-Science Reviews, v. 12, p. 1-33.

Swanberg, C. A., and Blackwell, D. D., 1973, Areal distribution and geophysical significance of heat generation in the Idaho batholith and adjacent intrusions in eastern Oregon and western Montana: Geol. Soc. Amer. Bull., v. 84, p. 1261-1282.

Talbot, J. L., and Hyndman, D. W., 1975, Consequence of subduction along the Mesozoic continental margin west of the Idaho batholith: Geol. Soc. Amer., Abstracts with Programs, v. 7, p. 1290.

Taylor, H. P., 1978, Oxygen and hydrogen isotope studies of plutonic granitic rocks. Earth Planet. Sci. Letters, v. 38, p. 177-210.

Thornton, C. P., and Tuttle, O. F., 1960, Chemistry of igneous rocks, I: Differentiation index: Amer. Jour. Sci., v. 258, p. 664-684.

Tuttle, O. F., and Bowen, N. L., 1958, Origin of granite in the light of experimental studies in the system $NaAlSi_3O_8$-$KAlSi_3O_8$-SiO_2-H_2O: Geol. Soc. Amer. Memoir 74, 153 p.

Umpleby, J. B., Westgate, L. G., and Ross, C. P., 1930, Geology and ore deposits of the Wood River region, Idaho: U.S. Geol. Survey Bull. 814, 250 p.

Vallier, T., 1977, The Permian and Triassic Seven Devils group, western Idaho and northeastern Oregon: U.S. Geol. Survey Bull. 1437, 58 p.

Vance, J. A., 1969, On Synneusis: Contrib. Mineral. Petrol., v. 24, p. 7-29.

von Backstrom, J. W., 1970, The Rossing uranium deposit near Swakopmund, South West Africa, in Uranium exploration geology: Vienna, Int'l. Atomic Energy Agency, p. 143-149.

_____ 1974, Other uranium deposits, in Formation of uranium ore deposits: Vienna, Int'l. Atomic Energy Agency, p. 605-620.

Whitney, J. A., 1975a, The effects of pressure, temperature, and X_{H_2O} on phase assemblage in four synthetic rock compositions: Jour. Geol., v. 83, p. 1-31.

_____ 1975b, Vapor generation in a quartz monzonite magma: a synthetic model with application to porphyry copper deposits: Econ. Geol., v. 70, p. 346-358.

Wilcox, R. E., 1979, The liquid line of descent and variation diagrams, in Yoder, H.S. (ed.), The evolution of the igneous rocks: Princeton, New Jersey, Princeton Univ. Press, p. 205-232.

Williams, H., Turner, F. J., and Gilbert, C. M., 1954, Petrography: an introduction to the study of rocks in thin section: San Francisco, Freeman, 406 p.

Williams, P. L., 1961, Glacial geology of Stanley Basin: Idaho Bur. Mines & Geol., Pamphlet 123, 29 p.

Winkler, H. G. J., 1979, Petrogenesis of metamorphic rocks (5th edition): New York, Springer-Verlag, 348 p.

Wiswall, G., 1979, Structure and petrography below the Bitterroot dome, Idaho batholith, near Paradise, Idaho: Ph.D. dissert., Univ. Montana, Missoula, 129 p.

Wright, H. D., and Bieler, B. H., 1960, Primary mineralization of uranium-bearing "siliceous reef" veins in the Boulder batholith, Montana: Part I - the host rocks: Econ. Geol., v. 55, p. 56-72.

Wyllie, P. J., Huang, W. L., Stern, C. R., and Maaløe, S., 1976, Granitic magmas: possible and impossible sources, water contents, and crystallization sequences: Can. Jour. Earth Sci., v. 13, p. 1007-1019.

York, D., and Farquhar, R. M., 1972, The earth's age and geochronology: New York, Permagon Press, 178 p.

APPENDIX I

Table A. Mineralogy and visual estimate of modes from thin sections of Cretaceous equigranular granite.

	K-feldspar	quartz	plagioclase	An (content)	biotite	opaques	apatite	sphene	zircon	Alteration minerals present:	chlorite	white micas	iron oxides
BB-52	20	25	40	(30)	10	2	t	2	t		x	x	x
BB-53	34	30	35	nd	1	-	t	-	t		-	x	x
BB-71*	25	35	37	(24)	.6	.3	t	t	-		-	x	x
PR-2	10	30	50	nd	8	2	-	t	-		-	x	-
PR-3	20	30	40	nd	7	-	t	t	-		-	x	-
RB-1	15	20	40	(26)	13	2	-	-	-		-	-	-

Sample Locations:

BB-52: Bell Cross prospect: center, section 10, T. 11 N., R. 13 E.

BB-53: Bell Cross prospect: center, section 10, T. 11 N., R. 13 E.

BB-71: West center, section 11, T. 11 N., R. 13 E.

PR-2: 18.6 miles east of Lowman on Idaho Highway 21.

PR-3: 8.8 miles east of Lowman on Idaho Highway 21.

RB-1: Between Robinson Bar and Peach Creek on Idaho Highway 75.

*2000 point counts.

Table B. Mineralogy and visual estimates of modes from thin sections of Cretaceous quartz granite porphyry.

	K-feldspar	quartz	plagioclase	An (content)	biotite	opaques	apatite	sphene	Alteration minerals present:	carbonate	white micas	iron oxides
BB-49	20	20	50	(29)	10	t	-	-		-	x	x
BB-61	10	35	40	(36)	10	t	t	-		x	x	x
BB-61a	14	25	45	(29)	8	3	-	t		x	x	-
BB-70*	50	26	20	(29)	3	0.5	-	-		-	x	x
BB-73*	10	42	39	(26)	7	t	-	-		x	x	-
EBC-8*	11	36	46	nd	6	2	t	-		-	x	x

Sample Locations:

BB-49: Baker prospect: southeast section 35, T. 12 N., R. 13 E.

BB-61: Lightning Number 2 prospect: center, section 1, T. 11 N., R. 13 E.

BB-61a: Lightning Number 2 prospect: center, section 1, T. 11 N., R. 13 E.

BB-70: Southeast, section 11, T. 11 N., R. 13 E.

BB-73: Lightning Number 2 prospect: center, section 1, T. 11 N., R. 13 E.

EBC-8: West center, section 6, T. 11 N., R. 14 E.

*2000 point counts.

Table C. Mineralogy and visual estimate of modes from thin sections of Cretaceous K-feldspar porphyritic granite.

	K-feldspar	quartz	plagioclase	An (content)	biotite	opaques	apatite	sphene	zircon	hornblende	Alteration minerals present:	white micas	chlorite	iron oxides	carbonate
BB-8	35	25	35	(22)	5	t	t	t	-	-		x	-	-	-
BB-43	50	25	15	nd	10	t	t	t	-	-		x	x	-	-
EBC-15*	36	27	29	(28)	6	t	t	t	-	-		x	x	-	-
EBC-24	40	25	35	(21)	1	1	-	-	t	-		x	-	-	-
EBC-25	20	30	45	nd	5	t	t	t	-	-		x	x	x	-
EBC-36	50	15	30	nd	5	t	t	t	-	-		x	-	-	x
EBC-46	10	35	45	nd	10	t	-	1	-	-		x	x	x	-
EBC-47*	13	35	42	nd	10	0.5	t	t	t	-		x	x	-	x
EBC-48*	25	33	31	(21)	9	0.1	t	t	-	-		x	x	-	x
EBC-49*	4	43	34	(22)	11	0.6	t	t	t	7		x	x	-	x
EBC-55	20	30	35	(35)	11	1	-	3	-	-		x	x	-	-
#11	40	10	35	(22)	10	t	t	2	-	2		x	x	-	-

Sample Locations:

BB-8: East center, section 12, T. 11 N., R. 13 E.
BB-43: Southwest of Sunday Creek and Basin Creek confluence.
EBC-15: Center, section 1, T. 11 N., R. 13 E.
EBC-24: Alta prospect: northwest, section 14, T. 11 N., R. 14 E.
EBC-25: Alta prospect: northwest, section 14, T. 11 N., R. 14 E.
EBC-36: Hardee prospect: southeast, section 10, T. 11 N., R. 14 E.
EBC-46: Hardee prospect: southeast, section 10, T. 11 N., R. 14 E.
EBC-47: Center, section 21, T. 11 N., R. 14 E., on Basin Creek road.
EBC-48: Southeast, section 23, T. 11 N., R. 14 E., on Idaho Highway 75.
EBC-49: Southwest, section 24, T. 11 N., R. 14 E., on Idaho Highway 75.
EBC-55: Northwest, section 28, T. 11 N., R. 14 E., on Idaho Highway 75.
#11: Immediately west of Sunbeam on Idaho Highway 75.

*2000 point counts.

Table D. Mineralogy and visual estimate of modes from thin sections of Cretaceous leucocratic granite.

	K-feldspar	quartz	plagioclase	An (content)	biotite	opaques	apatite	sphene	zircon	Alteration minerals present:	white micas	chlorite	iron oxides	carbonate
EBC-42	40	35	22	nd	3	t	-	-	-		x	-	x	-
EBC-43	25	35	40	(21)	t	t	-	-	-		x	-	x	x
EBC-52*	18	30	46	(24)	4	0.5	t	-	-		x	x	x	-
EBC-53*	37	30	27	(27)	2	1	-	-	-		x	x	x	-
#3	20	35	40	(22)	5	t	t	t	-		x	x	-	x
#9	10	35	45	(24)	10	t	t	t	t		x	x	-	-
#19	40	24	35	(24)	1	t	-	-	-		x	x	-	-

Sample Locations:

EBC-42: West center, section 20, T. 11 N., R. 14 E.

EBC-43: Center, section 20, T. 11 N., R. 14 E.

EBC-52: Center, section 20, T. 11 N., R. 14 E., on Idaho Highway 75.

EBC-53: Southeast, section 19, T. 11 N., R. 14 E.

#3: West center, section 29, T. 11 N., R. 16 E., on Idaho Highway 75, immediately west of Torreys Inn.

#9: West, section 21, T. 11 N., R. 15 E., on Idaho Highway 75, west of Stovepipe Spring.

#19: Northeast, section 35, T. 11 N., R. 13 E., on Idaho Highway 75, east of Joe's Gulch.

*2000 point counts.

Table E. Mineralogy and visual estimate of modes from thin sections of Cretaceous aplites and pegmatite dikes.

	K-feldspar	quartz	plagioclase	An (content)	biotite	opaques	muscovite	apatite	sphene	Alteration minerals present:	white micas	chlorite
EBC-41a	15	20	55	nd	7	3	t	t	t		x	-
EBC-41b	45	25	25	(20)	2	3	-	-	-		x	x
EBC-41c	40	25	30	(20)	3	t	t	t	-		x	x
EBC-41d	50	20	30	(24)	1	t	-	-	-		x	x

Sample Locations:

EBC-41a, b, c, d: Southeast, section 23, T. 11 N., R. 14 E., on Idaho Highway 75.

Table F. Mineralogy and visual estimate of modes from thin sections of Tertiary rhyolite.

	K-feldspar	quartz	plagioclase	An (content)	biotite	opaques	hornblende	muscovite	zircon	apatite	Alteration minerals present:	chlorite	white micas	clays	carbonate	iron oxides
BB-23	30	20	30	nd	t	1	-	t	-	-		x	x	x	-	-
BB-39	40	30	20	nd	2	2	2	-	t	t		x	x	x	x	x
EBC-51	60	25	10	(25)	1	t	-	t	t	-		5	x	x	x	-
A-4	60	20	t	nd	t	t	-	-	-	-		15	-	-	-	x

Sample Locations:

BB-23: Northeast, section 1, T. 11 N., R. 13 E.

BB-39: Northwest, section 1, T. 11 N., R. 13 E.

EBC-51: Southwest, section 21, T. 11 N., R. 14 E., on Idaho Highway 75.

A-4: South center, section 36, T. 12 N., R. 13 E.

Table G. Mineralogy and visual estimate of modes from thin sections of Tertiary silicic dikes.

	K-feldspar	quartz	plagioclase	opaques	Alteration minerals present:	white micas	carbonate
BB-18	25	40	30	t		5	-
BB-47	50	50	-	t		t	-
EBC-54	25	60	2	t		13	-
#18	45	45	-	1		5	1

Sample Locations:

BB-18: Center, section 12, T. 11 N., R. 13 E.

BB-47: Center, section 12, T. 11 N., R. 13 E.

EBC-54: West center, section 19, T. 11 N., R. 14 E.

#18: Center, section 36, T. 11 N., R. 13 E., on Idaho Highway 75.